Excess Vascular Endothelial Growth Factor-A Disrupts Pericyte Recruitment during Blood Vessel Formation

Jordan Darden[1,2], Laura Beth Payne[1], Huaning Zhao[1,3], John C. Chappell[1,2,3,4]

[1]Center for Heart and Regenerative Medicine, Virginia Tech Carilion Research Institute, Roanoke, VA 24016, USA

[2]Graduate Program in Translational Biology, Medicine, and Health, [3]Department of Biomedical Engineering and Mechanics, Virginia Polytechnic Institute and State University, Blacksburg, VA 24061, USA

[4]Department of Basic Science Education, Virginia Tech Carilion School of Medicine, Roanoke, VA 24016, USA

Running Title: Excess VEGF-A Disrupts Pericytes

Corresponding Author: John C. Chappell, Ph.D.
Virginia Tech Carilion Research Institute
2 Riverside Circle
Roanoke, Virginia 24016
Phone: 540-526-2219 / Fax: 540-982-3373
E-mail: JChappell@vtc.vt.edu

COI Statement: The authors have declared that no conflict of interest exists.

Keywords: pericyte, VEGF-A, angiogenesis, mouse embryonic stem cells, development

Abbreviations: NG2: Neural Glial Antigen-2. VEGF: Vascular Endothelial Growth Factor. ESC: Embryonic Stem Cell. PDGF: Platelet-Derived Growth Factor.

Abstract: 250 words
Manuscript (including Figure Legends, Methods and References): 10,422 words
Figures: 7
Supplemental Data: 2 Movies and 6 Figures

ABSTRACT

Pericyte investment into new blood vessels is essential for vascular development such that mis-regulation within this phase of vessel formation can contribute to numerous pathologies including arteriovenous and cerebrovascular malformations. It is critical therefore to illuminate how angiogenic signaling pathways intersect to regulate pericyte migration and investment. Here, we disrupted vascular endothelial growth factor-A (VEGF-A) signaling in *ex vivo* and *in vitro* models of sprouting angiogenesis, and found pericyte coverage to be compromised during VEGF-A perturbations. Pericytes had little to no expression of VEGF receptors, suggesting VEGF-A signaling defects affect endothelial cells directly but pericyte indirectly. Live imaging of *ex vivo* angiogenesis in mouse embryonic skin revealed limited pericyte migration during exposure to exogenous VEGF-A. During VEGF-A gain-of-function conditions, pericytes and endothelial cells displayed abnormal transcriptional changes within the platelet-derived growth factor-B (PDGF-B) and Notch pathways. To further test potential crosstalk between these pathways in pericytes, we stimulated embryonic pericytes with Notch ligands Delta-like 4 (Dll4) and Jagged-1 (Jag1) and found induction of Notch pathway activity but no changes in PDGF Receptor-β (*Pdgfrβ*) expression. In contrast, PDGFRβ protein levels decreased with mis-regulated VEGF-A activity, observed in the effects on full-length PDGFRβ and a truncated PDGFRβ isoform generated by proteolytic cleavage or potentially by mRNA splicing. Overall, these observations support a model in which, during the initial stages of vascular development, pericyte distribution and coverage are indirectly affected by endothelial cell VEGF-A signaling and the downstream regulation of PDGF-B-PDGFRβ dynamics, without substantial involvement of pericyte Notch signaling during these early stages.

INTRODUCTION

Each year, millions of patients are afflicted by pathological conditions that arise from structural abnormalities within the vascular system [1]. In particular, defective blood vessel formation within neurological tissues can increase patient risk for sudden, life-threatening events such as a stroke or aneurysm. Notable examples of these cerebrovascular disorders include arteriovenous malformations (AVMs), cerebral cavernous malformations (CCMs), and cerebral autosomal dominant arteriopathy with subcortical infarcts and leukoencephalopathy (CADASIL) [2-4]. In addition to these pathologies, vascular anomalies can pose severe health risks to pediatric patients, as poorly formed cerebrovasculature can lead to a hemorrhagic stroke and numerous related health consequences, particularly in premature infants [5]. Development of these blood vessels depends heavily on the precise integration of spatio-temporal cues and cellular responses to achieve proper vessel structure and patterning for adequate oxygen delivery and nutrient exchange.

Of the molecular signals that initiate and pattern new vessel formation, vascular endothelial growth factor-A (VEGF-A) is one of most potent, eliciting numerous downstream effects in vascular endothelial cells [6,7]. Inputs from additional signaling networks therefore modulate the pleiotropic effects of VEGF-A to coordinate endothelial cell migration [8], proliferation [9], and shape change [10], among other key behaviors. Crosstalk between the VEGF-A and Notch pathways, for example, is critical for a subset of endothelial cells to adopt a sprouting phenotype (i.e. an endothelial “tip” cell), while other endothelial cells trail behind these leading cells and proliferate to elongate the nascent vessel branch [11-13]. Disrupting this intersection between VEGF-A and Notch

signaling not only undermines endothelial sprouting, but also compromises downstream regulation of other pathways including the platelet-derived growth factor-B (PDGF-B) pathway [14,15]. PDGF-B signals are critical for promoting vascular network progression through the recruitment and expansion of mural cells i.e. vascular smooth muscle cells and pericytes [16]. These unique signaling interactions therefore orchestrate each stage of vessel formation, from mechanisms governing angiogenic sprouting and remodeling to those underlying vessel stabilization and maturation by mural cells.

Pericytes contribute to the development of mature vascular beds by maintaining endothelial cell junction integrity [17,18] and synthesizing extracellular matrix (ECM) components of the surrounding vessel basement membrane [19]. In addition to these more established roles, unique pericyte functions are still being discovered in normal and disease settings. For instance, pericytes in neural tissue may play a physiological role in blood flow distribution through vasocontractility [20,21], but this function may also go awry in certain pathological scenarios by contributing to limited tissue reperfusion following ischemia [22,23]. To perform these and other critical functions in sustaining tissue health, pericytes must establish sufficient coverage along the vasculature through their migration along and investment into the vessel wall [24]. These important cellular processes that promote pericyte coverage are also mediated, in part, by the intricate interplay between the signaling cascades described briefly above, that is, the VEGF-A, Notch, and PDGF-B pathways.

Notch and VEGF-A signaling have also been implicated in regulating pericyte behaviors

directly [25,26], but evidence suggesting a context-dependence for these pathways in pericytes [27-33], as well as their crosstalk with the PDGF-B pathway [4,34-39], highlights the need for further clarification of these signaling relationships. Pericytes express PDGF Receptor-β (PDGFRβ) on their surface to bind PDGF-B ligands and facilitate downstream intracellular signaling events [40]. Pericyte coverage therefore depends on competent PDGF-B signaling, as targeted disruption of this pathway leads to compromised pericyte investment within the vessel wall across many tissue beds [16,41-43]. Given the sensitivity of pericytes to PDGF-B signals, it is perhaps not surprising that soluble isoforms of PDGFRβ have recently been identified [44-47]. These observations suggest the existence of a negative feedback loop that modulates PDGF-B signaling to "fine-tune" pericyte behaviors in certain contexts, though this potential mechanism remains relatively unexplored.

In the present study, we utilized *in vitro* and *ex vivo* models of sprouting angiogenesis in which pericytes migrated along and expanded their coverage of developing blood vessels. Because of its critical role in vessel formation, we targeted VEGF-A signaling directly by manipulating Flt1 (VEGF Receptor-1), a negative regulator of VEGF-A that acts primarily as a "decoy" or ligand sink during vessel development [9,11]. Although Flt1 also binds Placental Growth Factor (PlGF) and VEGF-B, the intracellular tyrosine kinase domain of Flt1 is dispensable for normal vascular development [48], again supporting its function as a ligand trap. In addition, while VEGF-A signals through Flk1/Kdr (VEGF Receptor-2) on endothelial cells, Flt1 binds VEGF-A with a 10-fold higher affinity than Flk1/Kdr [49], consistent with a role in regulating available VEGF-A ligand. Genetic loss of *Flt1* in fact

leads to excessive and aberrant Flk1 activation via increased receptor phosphorylation, as observed in ESC-derived vessels and the developing postnatal mouse retina [8,9,50-54]. Disrupting VEGF-A activity genetically (*flt1*$^{-/-}$) or pharmacologically (exogenous VEGF-A) impaired pericyte distribution and coverage on the developing vasculature, with pericyte migration being restricted during exposure to elevated VEGF-A levels. These VEGF-A gain-of-function scenarios [9,50-53] led to abnormal transcriptional changes within the Notch and PDGF-B pathways in both pericytes and endothelial cells. Although these transcriptional irregularities suggested potential connections between these two pathways, we found that stimulating embryonic pericytes with Notch ligands [Delta-like 4 (Dll4) and Jagged-1 (Jag1)] did not alter *Pdgfrβ* expression. We did however observe a decrease in PDGFRβ protein levels during disrupted VEGF-A activity and specifically in the levels of a truncated PDGFRβ isoform. These PDGFRβ isoforms have been detected in a number of settings [44-47,55], and their relative amounts appear to vary with corresponding PDGF-B levels and potentially with proteolytic cleavage events [45], though mRNA splice variants cannot be ruled out. Overall, these data demonstrate that, in early developmental blood vessel formation, pericyte distribution and coverage depend on proper VEGF-A activity and its downstream impact on PDGF-B-PDGFRβ dynamics, without substantial involvement of the Notch pathway during these initial stages.

MATERIALS AND METHODS

Cell Culture and In Vitro Differentiation

WT and *flt1*$^{-/-}$ mouse embryonic stem cells (ESCs) were a gift of V.L. Bautch (University of North Carolina at Chapel Hill) and Guo-Hua Fong (University of Connecticut). Undifferentiated cells were maintained through leukemia inhibitory factor (LIF) exposure as described previously [56]. After undifferentiated WT and *flt1*$^{-/-}$ ESCs gave rise to spherical embryoid bodies (EBs) (i.e. over 3-4 days in culture), these EBs were released from the culture plate and collected using 1x dispase (Gibco, Cat #17105-041) in PBS (i.e. experimental Day 0). EBs were washed twice with PBS and re-plated in differentiation media (see Online Resource 1 – Supplemental Materials and Methods) in 10 cm^2 petri dishes (i.e. non-tissue culture treated plastic). The cell suspension in media was added at 5 mls per plate and cultured at 37^{o}C and 5% CO_2. On experimental Day 3 (i.e. 3 days after dispase), EBs were transferred to slide flasks (ThermoFisher, Cat #170920) using sterile wide-tip transfer pipets. Differentiating EBs were cultured for a 5-7 additional days, feeding at Days 5 and 8, for a total of 8-10 days. Differentiated cells were washed twice with PBS and processed for (i) immunocytochemistry (ICC) and confocal imaging or (ii) cell-type enrichment and transcriptional profiling by quantitative Real-Time PCR (qRT-PCR).

Immunocytochemistry and Quantitative Image Analysis

Differentiated ESCs were fixed at designated end-points with either (i) 50:50 solution of methanol and acetone for 6 mins, or (ii) 4% paraformaldehyde (PFA) for 5 mins. Samples were stored in PBS at 4^{o}C until further processing. Immunostaining of differentiated

ESCs in slide flasks was performed with the following primary antibodies: rabbit anti-neural glial antigen-2 (Ng2, EMD Millipore, Cat #AB5320), rat anti-platelet-endothelial cell adhesion molecule-1 (Pecam1/CD31, BD Pharminogen, Cat #553370), and mouse anti-β-Galactosidase (β-Gal, ThermoFisher, Cat #MA1-152). Secondary antibodies included: donkey anti-rat AlexaFluor 488 (Jackson Immunoresearch, Cat #705-545-147), donkey anti-rabbit AlexaFluor 568 (Invitrogen, Cat #A10042), and donkey anti-mouse AlexaFluor 647 (Abcam, Cat #ab150107). Cell nuclei were labeled with 4′,6-Diamidino-2-phenylindole dihydrochloride (DAPI, Sigma, Cat #D9542). All antibodies were used at a 1:1000 concentration. Fixed ESCs were washed twice with PBS, and non-specific antigens were blocked with a 3% bovine serum albumin (BSA, Sigma, A2153-100G) solution in PBS (with 0.01% sodium azide as a preservative) at room temperature for 1 hour. Samples were incubated in primary antibody solutions overnight at 4°C followed by PBS washes (3x with 10 mins per wash). Secondary antibodies plus DAPI were incubated for 4 hours at room temperature followed by 3 more PBS washes. After PBS was aspirated, slide flask chambers were removed, and a line of Vectashield mounting media (Vector Labs, Cat #H-1000) was applied on the culture area. A cover slip was applied (22 mm x 60 mm – 1.5 thickness, ThermoFisher, Cat #12-544G), and slides were sealed with clear nail polish (Electron Microscopy Sciences, Cat #72180).

Differentiated ESCs were imaged with a Zeiss LSM880 confocal microscope using a 40x water objective. Images were collected in 5-30 confocal scans through the z-axis and flattened. Image analysis was conducted with ImageJ/FIJI software available for download at https://fiji.sc/ [57]. Ng2+ cells were assessed visually in three dimensions to confirm

direct association with Pecam1+ endothelial cells, and those not clearly associated with developing vessels were excluded from pericyte coverage analysis. Color channels were separated, and Pecam1+ endothelial cell area was determined through application of a pixel intensity threshold value. Regions of overlaps between Ng2+ signal and Pecam1+ endothelial cells were established, and pixel areas of these overlapping regions were measured. Percent of pericyte coverage was calculated by dividing the area of Ng2+ overlap with Pecam1+ cells by the total Pecam1+ vessel area. FIJI plugin cell counter and fixed diameter macros were used to analyze the distribution of Ng2+ pericytes throughout the ESC-derived vasculature. Ng2+ pericyte distributions were measured relative to (i) vessel morphological features (i.e. vessel stalks, branch points, or thicker areas) and (ii) other Ng2+ cells in close proximity (i.e. within a 50-micron radius).

Endothelial Cell and Pericyte Enrichment

Mouse WT and *flt1*$^{-/-}$ ESCs were differentiated for 10 days on tissue culture-treated 10 cm^2 plates (Corning, Cat #430167) per cell type. Pericytes and endothelial cells were enriched from ESC cultures using magnet-assisted cell sorting (MACS) (Miltenyi Biotec), as described previously [11]. Briefly, cells were dissociated through incubation in 7 mL of a 50:50 solution of dispase (2x) and type 1 collagenase (Fisher, Cat #NC9633623) at 37^{o}C for 40 minutes. Cultures were also mechanically dissociated by pipetting until in suspension. The resultant cell suspension was then filtered (70-micron bucket filter) to yield single cells, which were centrifuged and dissociation enzymes aspirated. Cells were resuspended in autoMACS® running buffer (Miltenyi Biotec, Cat #130-091-221). Fc-Receptor blocking reagent (Miltenyi Biotech, Cat #130-092-575) was added per

manufacturer instructions and incubated for 20 mins at 4°C, agitating each tube every 5 mins. After centrifugation and supernatant aspiration, cells were resuspended in autoMACS® buffer containing anti-An2 microbeads (Miltenyi Biotec, Cat #130-097-170). An2 is a homologue of Ng2 [58]. Additionally, microbeads were 50-nm superparamagnetic particles, avoiding cell stimulation. Following centrifugation, aspiration of microbead solution, and resuspension in autoMACS® buffer, labeled cells were manually passed through QuadroMACS separator LS columns (Miltenyi Biotec, Cat #130-091-051, 30-micron pre-separation filters) per manufacturer recommendations. Cells flowing through the column but not isolated by the magnetic field were collected for secondary selection of endothelial cells. After centrifugation of these "flow-through" cells, sorting buffer was aspirated, and cells were resuspended in MACS® buffer. Following incubation with Pecam1/CD31 primary antibodies conjugated to R-phycoerythrin (PE) (BD Pharminogen, Cat #553373), cells were then incubated with anti-PE microbeads, as described above. After each MACS column separation, target populations were collected, as well as the final "flow through" cells, all of which were centrifuged and resuspended in buffers formulated for additional analysis of mRNA transcripts (TRIzol, Invitrogen, Cat #15596018) or protein [radioimmunoprecipitation assay (RIPA) buffer].

Transcription Analysis by Quantitative RT-PCR

We chose day 10 for our transcriptional analysis with the prediction that gene expression changes might be more pronounced and potentially cumulative, reflecting the decrease in pericyte coverage. Endothelial cell and pericyte-enriched mRNA samples were extracted and purified using Quick-RNA MiniPrep kits (Zymo Research, Cat #R1055) following

manufacturer instructions. Reverse transcription of mRNA to cDNA was achieved using SuperScript® VILO™ and RNase H reagents (Invitrogen Cat #11754-050 and #18021-071, respectively) and following manufacturer instructions. Quantitative RT-PCR was conducted in triplicate utilizing Taqman® Universal Master Mix II, with UNG (Life Technologies, Cat #4440038). "Best Coverage" murine Taqman® probes for gene expression analysis (Applied Biosystems, ThermoFisher) included primers for TATA binding protein (*Tbp*, for expression normalization) and the following targets: *Flt1*, *Dll4, Jag1, Notch1, Notch3, Hes1, Hey1, Hey2, HeyL, Pdgf-b, Perlecan/Hspg2,* and *Pdgfrβ*. Samples were run in Standard 96-well plates on a QuantStudio6 Flex (Applied Biosystems, ThermoFisher), and results processed with QuantStudio Expression qRT-PCR software applying comparative ΔΔT method to determine expression changes.

Live Imaging of Ex Vivo Angiogenesis and Quantitative Movie Analysis

All animal experiments were conducted with review and approval from the Virginia Tech IACUC. All protocols were reviewed and approved by IACUC boards. The Virginia Tech NIH/PHS Animal Welfare Assurance Number is A-32081-01 (expires 7/31/2021). Embryonic tissue culture assay (ETCA) experiments were conducted as previously described [50]. Briefly, following mating with *Flk1-eGFP; Ng2-DsRed* males, pregnant C57BL/6 female mice were sacrificed at embryonic day 14.5 (E14.5) by CO_2 inhalation and cervical dislocation. Embryos were retrieved from the uterus in 4ºC dissection media, and genotype was evaluated by fluorescence microscopy. Embryos positive for both *Ng2-DsRed* (i.e. pericyte signal) and *Flk1-eGFP* (i.e. endothelial cell signal) were selected for micro-dissection to isolate dorsal skin (i.e. tissue absent of Ng2+ glia). Dermal tissues

were placed in single wells of a glass-bottom 6-well plate and embedded in a fibrin matrix with the hypodermis (subcutaneous layer) facing the glass. Basic culture media was added at 3 mL per well. The following day, spent media was replaced with culture media containing PBS (vehicle control) or VEGF-A (50 ng/ml, Peprotech, Cat #450-32). Plates were then transferred to an incubation chamber (37^{o}C, 5% CO_2, humidity controlled) mounted on a Zeiss LSM880 confocal microscope for live imaging. Multi-position, time-lapse confocal scans were acquired through each sample thickness (z-stacks: 6-8 images with 4-6 microns between planes) at 10-25 minute intervals for a minimum of 12 hours using a 20x objective. Each time point was compressed from the raw z-stack and exported as a video file in RGB channel format. Representative movie sequences shown are from non-consecutive images.

Movies of ex vivo blood vessel development in the ETCA experiments were analyzed for pericyte migration during control and VEGF-A-treated conditions. Pericyte migration was classified as persistent in a particular direction ("Directional Persistence") or static without movement in a clear direction ("Static Movement"). In addition, *Ng2-DsRed*+ pericyte distribution was evaluated at the beginning and end of each movie sequence by quantifying the number of neighboring pericytes within a 50-micron radius.

Embryonic Pericyte Culture on Immobilized Notch Ligands

In a separate study, Ng2-DsRed+ pericytes were isolated from embryonic mice at E12.5 and validated by standard approaches as well as in functional assays (see Online Resource 1 – Supplemental Materials and Methods) [59]. These cells were grown to

confluence before enzymatic release and cultured on Notch ligand-coated plates. Ligand-coated plates were prepared by applying AffiniPure mouse anti-human IgG (Fcγ fragment specific, Jackson ImmunoResearch, Cat #209-005-098) to 10 cm^2 cell culture dishes (Corning, Cat #430167) overnight at 37°C. Plates were washed twice with PBS (10 mins / wash), and non-specific epitopes were blocked with 10% FBS (Gibco) in PBS for 2 hours at room temperature in a cell culture hood. This blocking solution was aspirated, and each plate was treated overnight at 37°C with PBS (control), 10% FBS in PBS blocking solution (serum block control), or 50 nM of one of the following: Human IgG only control (Fc fragment, Jackson ImmunoResearch, Cat #009-000-008), Recombinant rat Jagged-1-human IgG Fc chimera protein (R&D Systems, Cat #599-JG-100), or Recombinant mouse Dll4-human IgG Fc chimera protein (Adipogen, Cat #AG-40A-0145-C050). Plates were then washed twice with PBS (10 mins / wash), and pericytes were added to each plate condition in pericyte media. Media was replenished 3 days after plating, and mRNA was collected in lysis buffer after 2 more days (i.e. cultured in each condition for 5 days total). RNA isolation, reverse transcription, and qRT-PCR was conducted as described above, applying the TaqMan probes (gene expression analysis) for: *Tbp*, *Hes1*, *Hey1, Hey2, HeyL, Notch1, Notch3,* and *Pdgfrβ.*

Protein Analysis

Western blot analysis was performed on cell lysates from MACS-enriched cell populations from ESC cultures differentiated for 10 days. Protein from ESC-derived endothelial cells and pericytes was collected in RIPA buffer. DC Protein Assay with Reagents A, S, and B

(Bio-Rad) facilitated quantification of protein concentrations for each sample. Protein samples of equivalent concentration were separated by SDS-PAGE in standard running buffer (Bio-Rad) on 4-15% Mini PROTEAN® Pre-cast TGX gels (Bio-Rad, Cat # 456-1086). Separated proteins were transferred to Immobilon-FL PVDF Membrane for fluorescent and chemifluorescence (EMD Millipore, Cat # IPFL00010). Blocking solution [5% BSA in Tris-buffered solution with 0.1% Tween 20 (TBS-T)] was applied to membranes overnight at 4°C. Primary antibodies were incubated overnight at 4°C on a rotator. After washing 4x with TBS-T, secondary antibodies were incubated for 2 hours at room temperature. Following 4 washes with TBS-T, membranes were imaged on a ChemiDoc system (BioRad). Primary antibodies included: goat anti-Pdgfrβ (R&D Systems, Cat #AF1042) and rabbit anti-GAPDH (Abcam, Cat #ab9485). Recombinant Pdgfrβ (R&D Systems, Cat #1042-PR-100) was also run on a gel, transferred, and immunostained to validate primary antibody specificity. Secondary antibodies used were: donkey anti-goat AlexaFluor 488 (Jackson ImmunoResearch Cat #705-545-003), and donkey anti-rabbit AlexaFluor 647 (Jackson ImmunoResearch Cat #711-605-152) at recommended dilutions. Relative protein levels were evaluated using BioRad Image Lab 5.1.

Pdgfrβ Isoform Characterization by PCR and Gel Electrophoresis

Targeted regions of cDNA derived from MACS-enriched An2+ pericyte samples were amplified via PCR using Taq Core Kit (Qiagen, Cat #201225). Amplicons were separated by gel electrophoresis using 2% agarose in Tris-acetate-EDTA buffer with SYBR Safe DNA gel stain (Invitrogen, Cat #S33102). Fragment bands were visualized by UV

excitation. Primer sequences were designed using PrimerQuest, mapped in LaserGene, to target short fragments (<850bp) of mouse Pdgfrβ (*Mus musculus,* accession number NM_001146268).

	Forward	Reverse
Exons 1-5	5'- ACATCAGAAGCCATCTGTAGC-3'	5'-CGGATGGTGATGCTCTCG-3'
Exons 5-10	5'- GCAATGATGTGGTGAACTTCC-3'	5'- CGTTTCTAGCTGGCTCTCC3'
Exons 10-16	5'-TGGGAGGAAGATCAGGAATACG-3'	5'- CTCCTTTCATGTCCAACATGGG-3'
Exons 16-21	5'- CAAATACGCAGACATTGAGTCC-3'	5'- ATAGCCTTCACCCAGAAGC3'
Exons 21-23	5'- GAGGCTTCTGGGTGAAGG-3'	5'- GTAGAGCAATCCAGCTGAGG-3'

Statistics

Using GraphPad Prism 6 software, statistical analysis by Student's two-tailed t-test was applied to pericyte coverage and distribution measurements as well as to pericyte migration and distribution measurements from ETCA live imaging observations. Relative changes in gene expression (as quantified by qRT-PCR) were analyzed statistically using pair-wise Student's two-tailed t-tests. P-values less than or equal to 0.05 were considered significant.

RESULTS

Pericyte coverage and distribution depend on *Flt1* expression during early blood vessel formation.

Flt1 provides essential regulation of VEGF-A signaling to coordinate a range of endothelial cell behaviors during discrete stages of blood vessel branching [11,50,60,61]. Recent studies have suggested that, in addition to its unique roles in a variety of angiogenic contexts [62-65], Flt1 may directly or indirectly impact vascular mural cells during blood vessel maturation [27,28,66-68]. Here, we hypothesized that a VEGF-A gain-of-function, through genetic loss of *Flt1*, disrupts mechanisms facilitating pericyte-endothelial crosstalk such that early pericyte coverage and distribution along newly forming vessels are also impaired. Mouse embryonic stem cells (ESCs) give rise to numerous cell types when differentiated in the absence of specific cues to induce a particular lineage [56]. Endothelial cells organize into primitive vessel-like structures and ramify into larger networks through initial vasculogenic coalescence, subsequent angiogenic sprouting and anastomosis, and ultimately lumen formation, comparable to the progression of vascular development seen *in vivo* [69]. We observed ESC-derived vessels in WT and *Flt1*$^{-/-}$ cultures via immunostaining for platelet-endothelial cell adhesion molecule-1 (Pecam1) 8-10 days after the start of differentiation. *Flt1*$^{-/-}$ ESC-derived vessels were overgrown and poorly branched as compared to WT vessels (Figure 1), consistent with previous observations from this model [9,11,50,61]. *Flt1*$^{-/-}$ ESC-derived vessels also suffer from elevated and aberrant Flk1 phosphorylation and activation, as previously shown [9,50-53]. To identify vascular pericytes within these networks, we selected neural glial antigen-2 (Ng2; chondroitin sulfate proteoglycan-4, Cspg4) as our target for immunolabeling (Figure 1). This molecule is a well-accepted marker for

pericytes [70], is only expressed by other cell types such as oligodendrocyte precursors (OPCs) at later stages of development [71], and poses fewer challenges in cell type identification as compared to labels such as alpha-smooth muscle actin (aSMA; Acta2) and Desmin (Des) [70]. In WT vessels, Ng2+ pericytes were prevalent at vessel branch points, as often observed *in vivo* [72], as well as along vessel lengths and thicker vessels (Figures 1 and 2). In contrast, pericytes on *Flt1*$^{-/-}$ vessels were less numerous, exhibiting a significant reduction in overall vessel coverage and particularly at branch point and vessel length locations (see Online Resource 2 – Supplemental Figure 1 for additional representative images of distinct morphological locations for each genotype). Pericytes in the WT context steadily became more widespread over time (Figures 1 and 2), as their density within a 50-micron radius of one another steadily decreased. This shift in pericyte distribution may reflect recent observations of pericytes establishing their own unique "domains" of vessel coverage and avoiding spatial overlap [73]. Changes in pericyte density along *Flt1*$^{-/-}$ vessels were however more variable over time and displayed a later-stage trend towards increased accumulation i.e. more pericytes within a 50-micron radius of each other (Figure 2). To exclude the potential involvement of Placental Growth Factor (PlGF) and VEGF-B, which can also bind to Flt1 [74], we exposed WT ESC-derived vessels to ectopic VEGF-A and found a similar reduction in pericyte coverage (Online Resource 1 for experimental details, and Online Resource 3 – Supplemental Figure 2 for results). Taken together, these observations suggest that the loss of Flt1 activity and a gain-of-function for VEGF-A impairs pericyte distribution along nascent vessels such that pericyte coverage cannot match new vessel growth, likely due to direct effects on endothelial cell signaling that lead to a disconnect in mechanisms underlying pericyte-endothelial crosstalk.

Pericytes along nascent ESC-derived vessels lack *Flt1* expression.

Based on our observation of disrupted pericyte coverage and distribution on *Flt1*$^{-/-}$ vessels, we then tested the hypothesis that, in addition to endothelial cells [61], pericytes might also express *Flt1*, and their behavior may be directly affected by this genetic deletion. *Flt1* expression by vascular pericytes and mural cells remains an open question in the field, with contrasting observations across various models [27-33]. Our *Flt1*$^{-/-}$ ESCs express the *LacZ* reporter gene under the control of the endogenous *Flt1* promoter, thus providing a means to observe which cells actively express the *Flt1* gene. Immunostaining ESC-derived vessels for β-galactosidase, the product from the *Flt1-LacZ* gene, along with Ng2 labeling, demonstrated that Ng2+ pericytes had little to no *Flt1* gene activity relative to neighboring endothelial cells (Figure 3 and Online Resource 4 – Supplemental Figure 3). To further test for pericyte expression of *Flt1*, we used magnetic-activated cell sorting (MACS) to isolate and enrich for WT pericytes and endothelial cells from day 10 ESC-derived vessels, as described previously [11,75]. Using qRT-PCR for gene expression analysis, we found that WT pericyte expression of *Flt1* was significantly lower relative to WT endothelial cells in our differentiated ESCs (Figure 3 and Online Resource 4 – Supplemental Figure 3). Additional analysis of *Flk1/Kdr* (VEGF Receptor-2, VEGFR2) expression revealed that WT ESC-derived pericytes have little to no expression of this VEGF receptor relative to endothelial cells, which was verified further using our recently derived embryonic pericyte cell line (see Online Resource 4 – Supplemental Figure 3). Our data suggest that pericytes do not express appreciable levels of *Flt1* or *Flk1*, if any, during the early stages of vessel formation that we observed within our model. These results are consistent with previous observations from other developing vascular beds

[29-33], though pericyte *Flt1* expression may potentially be stage or model specific [27,28]. Furthermore, these observations suggest that *Flt1* loss likely results in direct disruption of endothelial cell signaling and that downstream effects on pericyte dynamics and coverage presumably occur indirectly, as pericytes express few to no VEGF receptors and therefore are unlikely to experience relevant levels of VEGF-A signaling.

Excess VEGF-A limits pericyte distribution by disrupting pericyte migration along sprouting endothelial cells.

Increased pericyte clustering, along with reduced pericyte coverage and distribution on developing *Flt1*$^{-/-}$ vessels, suggested that limited pericyte migration might be one of the primary defects caused indirectly by the loss of Flt1 regulation of the VEGF-A signaling in endothelial cells. To test this idea, we utilized an *ex vivo* model of early vessel formation that permitted real-time observation of pericyte and endothelial cell dynamics in the angiogenic context, as described previously [50]. Specifically, we used time-lapse confocal imaging to observe *Flk1-eGFP*+ endothelial cells and *Ng2-DsRed*+ *(Cspg4-DsRed+)* pericytes within the developing vasculature of explanted mouse embryonic skin [embryonic day 14.5 (E14.5)]. Angiogenic sprouting of *Flk1-eGFP*+ endothelial cells occurred during vehicle control treatment, with more robust sprouting observed in the VEGF-A-treated cultures (Figure 4). Additional analysis confirmed this increase in endothelial cell sprouting and revealed a net decrease in vessel branching for cultures exposed to ectopic VEGF-A (see Online Resource 5 – Supplemental Figure 4). Although no statistically significant differences were detected, these results were consistent with previous observations of *Flt1*$^{-/-}$ vessel dysmorphogenesis and the accumulation of remodeling defects [9,11,50,76]. Under vehicle control conditions, pericytes associated

with sprouting endothelial cells migrated in a persistent manner towards the direction of the extending sprout. In contrast, ectopic VEGF-A caused pericyte migration to become more static and randomized and much less directed towards endothelial cell sprouting and anastomotic connection events (Figure 4). VEGF-A-induced defects in pericyte migration were also reflected in the observation that pericyte density within a 50-micron radius increased from the first movie frame to the last (Figure 4). These data further highlight that mis-regulated VEGF-A signaling stunts pericyte coverage and distribution likely by severing the crosstalk among mechanisms coordinating endothelial cell formation of new vessels with pericyte expansion along a developing vascular network.

Loss of *Flt1* leads to dysregulated gene expression in the Notch and PDGF-B pathways.

During the initial stages of sprouting angiogenesis, endothelial cells integrate VEGF-A signals with cues received from neighboring endothelial cells, primarily via the Notch pathway [11-13], to establish an emerging “tip” cell and proliferative “stalk” cells. As the endothelial “tip” cell migrates outward from an existing vessel, it up-regulates production of PDGF-B [14,16,15], which is localized in the surrounding extracellular matrix (ECM) by heparin sulfate proteoglycans (HSPGs) [16,77,78]. We therefore hypothesized that losing Flt1 regulation of VEGF-A activity in endothelial cells leads to mis-regulation within the Notch and PDGF-B pathways; these gene expression defects in turn likely contribute to impaired pericyte-endothelial cell crosstalk and potentially lead indirectly to the observed reduction in pericyte coverage. As described above, we used MACS to obtain endothelial cells and pericytes from day 10 WT and *Flt1*$^{-/-}$ ESC-derived vessels. Gene expression

analysis by qRT-PCR revealed that, as reported previously [11], *Flt1*$^{-/-}$ endothelial cell expression of the Notch ligand *Dll4* was significantly increased, as were the downstream Notch-regulated transcription factors *Hes1*, *Hey1*, and *Hey2* (Figure 5). Transcripts for the Notch receptors *Notch1* and *Notch3* and the transcription factor *HeyL* were unchanged in *Flt1*$^{-/-}$ endothelial cells, which aligns with previous reports from various populations of endothelial cells exposed to excess VEGF-A [79]. In addition, we observed a significant decrease in endothelial expression of *Jagged1 (Jag1)* in *Flt1*$^{-/-}$ vessels, suggesting a down-regulation of this Notch ligand that has been implicated in mediating endothelial cell-mural cell crosstalk [4,38,34,35]. In contrast, *Flt1*$^{-/-}$ pericytes showed no significant changes in Notch pathway gene expression, though *Notch1*, *Hey1*, and *HeyL* displayed trends towards increased expression (Figure 5). In exploring the PDGF-B pathway, we found that expression levels of the ligand *Pdgfb* and the associated anchoring protein *Hspg2* (*Perlecan*) were significantly increased in *Flt1*$^{-/-}$ endothelial cells relative to WT, consistent with previous observations of endothelial cells in elevated VEGF-A environments [14]. Interestingly, we found that pericytes from *Flt1*$^{-/-}$ ESC-derived vessels had decreased expression of *Pdgfrβ* (PDGF Receptor-β gene) relative to WT pericytes. Collectively, these observations demonstrate that the genetic loss of *Flt1*, which is known to disrupt VEGF-A signaling in endothelial cells [9], has downstream effects on the Notch and PDGF-B pathways, likely disrupting signals that intersect or contribute indirectly to regulating pericyte coverage of developing blood vessels.

Pericytes produce a truncated PDGFRβ isoform during ESC-derived vessel formation.

Recent evidence suggests that vascular pericytes differentially regulate PDGFRβ depending on the particular microenvironment, such as during hypoxia, nutrient deprivation, or increased cell proliferation [44-47,55], consistent with our own data from the developing postnatal mouse brain (J. Darden and C. Jenkins-Houk, unpublished data). In observing altered *Pdgfrβ* transcriptional regulation in *Flt1*$^{-/-}$ ESC-derived pericytes, we hypothesized that these PDGFRβ isoforms, which may arise independent of Notch signaling [45], might be the more predominant PDGFRβ species in our ESC-derived vessels. To test this hypothesis and concurrently assess the relationship between PDGFRβ transcriptional changes and protein levels, we dissociated day 10 WT and *Flt1*$^{-/-}$ ESC-derived vessels, enriched for pericyte and endothelial populations using MACS as described above, and collected protein for Western Blot analysis. After using recombinant PDGFRβ to validate that our antibody was capable of detecting this protein (Figure 6), we applied this PDGFRβ antibody to detect PDGFRβ isoforms and their respective levels in each of our cell populations under WT and *Flt1*$^{-/-}$ conditions. Interestingly, we found an ~60 kDa PDGFRβ isoform present in both WT and *Flt1*$^{-/-}$ pericyte populations, with *Flt1*$^{-/-}$ pericytes containing around 3-fold less full-length PDGFRβ and this PDGFRβ isoform compared to WT pericytes (Figure 6).

In observing the differential regulation of this PDGFRβ isoform, we next asked how this isoform might be generated such as through alternative splicing on the mRNA level or post-translational cleavage as suggested by several previous studies [44-47]. We examined pericyte cDNA derived from ESC-derived vessel lysates for the presence of alternative splice variants. Specifically, we designed primer sets to amplify short, multiple exon-spanning regions of the complete, full-length *Pdgfrβ* transcript. PCR amplification

with primers spanning exons 1-5 produced two distinct bands when separated by gel electrophoresis, with migration bands corresponding to the expected ~730bp (full-length PDGFRβ) and a smaller ~370bp. All other PCR fragments yielded a single band of expected size. This indicates an alternative splice variant that is modified within the first 5 exons of PDGFRβ, likely coding for a shorter N-terminus or a skipped exon. This is consistent with a human PDGFRβ transcript variant that yields a shorter N-terminus (accession number NM_001355016). Sanger sequencing of these bands indicated skipping of exons 2 and 3 in the smaller band, which corresponds to loss of the PDGF-B binding domain of the transcribed protein (Figure 6). Functional relevance of such a splicing event suggests loss of PDGF-B ligand binding, although more extensive analyses on the protein and mRNA levels are needed. However, this spice variant (shorter by ~360bp) does not correspond to a ~60kDa translated protein. While the primer sets tested would likely detect a shorter mRNA variant due to exon skipping, they may not detect a truncated 3'-end variant. Therefore, the shorter protein isoform observed may be due a truncated transcript or translational cleavage. Further investigation is needed to determine the exact mechanism. Hutter-Schmid and Humpel (2016) demonstrate that cleavage modifications may actually be PDGF-B-dependent, consistent with *Pdgfb* transcriptional changes described above (Figure 5).

Embryonic pericytes respond to stimulation by immobilized Dll4 but not Jag1, but neither ligand induces changes in *Pdgfrβ* transcription.

Pericytes and smooth muscle cells engage in Notch signaling across a range of developmental contexts to promote their differentiation and augment overall vessel

maturation [4,38,34,35,37]. While Notch signals have been implicated in pericyte recruitment through regulation of *Pdgfrβ* expression [38,39], not all Notch pathway manipulations alter pericyte *Pdgfrβ* expression and impair pericyte coverage [35,36]. Observing lower *Jag1* expression in *Flt1*$^{-/-}$ endothelial cells and a concomitant decrease in *Pdgfrβ* expression in *Flt1*$^{-/-}$ pericytes suggested that Jag1 might regulate pericyte PDGFRβ in our model. Thus, a loss of Jag1 stimulation might impair embryonic pericyte migration and recruitment via reduced PDGFRβ activity. We tested this hypothesis using a functionally validated pericyte cell line recently derived in our lab from embryonic day 12.5 (E12.5) mice harboring the *Ng2-DsRed* reporter gene [59]. To stimulate Notch signaling in these embryonic pericytes, we cultured them on substrates of immobilized Dll4 or Jag1 as previously described [80-82], as well as on control substrates (untreated plate, Fc-γ with blocking serum only, and Fc-γ with human IgG, Fc fragment). Pericytes stimulated by immobilized Dll4 displayed significant increases in the downstream Notch targets *Hey1*, *Hey2*, and *HeyL* (notably a more than 35-fold increase), though not *Hes1*, and *Notch1* receptor transcription was also up-regulated (Figure 7). Jag1 ligands influenced pericyte transcription levels of downstream Notch targets, though statistically significant changes were not detected, and neither Dll4 nor Jag1 induced any changes in *Pdgfrβ* transcription. These results indicate that Dll4, but not Jag1, can stimulate Notch signaling in embryonic pericytes, but neither Notch ligand induces increased *Pdgfrβ* gene expression in these pericytes. To gain further insight into the potential role, or lack thereof, for Notch signaling in regulating pericyte coverage during early vessel formation, we exposed our WT and *Flt1*$^{-/-}$ ESCs to a Notch inhibitor during vessel formation (see Online Resource 1 – Supplemental Materials and Methods). We found that Notch

inhibition had no effect on pericyte coverage in either background (see Online Resource 6 – Supplemental Figure 5), further supporting the notion described in previous studies [35,37] that, at early stages in vessel development, pericyte coverage may not require Notch signaling.

DISCUSSION

Pericytes are critical components in the maturation of developing blood vessels into stable, higher-order vascular networks. In the current study, we show that mis-regulated VEGF-A signaling in endothelial cells indirectly compromises pericyte distribution and coverage along developing embryonic vessels, in part, by limiting pericyte migration. Defective VEGF-A regulation perturbed the Notch and PDGF-B pathways in both endothelial cells and pericytes, though direct stimulation of embryonic pericytes with Notch ligands did not affect *Pdgfrβ* expression. Interestingly, the indirect reduction in pericyte PDGFRβ that occurred with disrupted endothelial VEGF-A signaling was also detected on the protein level, that is, decreased levels of both full-length and truncated PDGFRβ isoforms. These PDGFRβ isoforms have been identified in unique biological contexts [44-47,55], and their relative abundance appears to be dependent on PDGF-B levels and proteolytic cleavage events [45], which is consistent with results from the current study. Taken together and summarized in Online Resource 7 – Supplemental Figure 6, these observations suggest pericyte coverage of developing vessels requires precise coordination of endothelial VEGF-A signaling, as this pathway provides important downstream regulation of pericyte distribution via PDGF-B-PDGFRβ activity, in a seemingly Notch-independent manner during early developmental stages.

Pericytes perform a broad range of functions in modulating blood vessel formation and remodeling [83-85], with new roles still being discovered [86,87]. Pericytes have been shown to directly and indirectly regulate VEGF-A signaling during vascular development, in part, via production of the VEGF receptor Flt1 [66,27,67,68], though this regulation

appears to be largely context dependent [28-32]. Our expression analysis of pericytes within ESC-derived vasculature indicated that these cells lack *Flt1* and *Flk1* expression levels comparable to that of endothelial cells at early embryonic time points. In another developmental model, a similar *in vivo* analysis of *Flt1* promoter activity [i.e. $Flt1^{lacZ/+}$ gene yielding β-galactosidase (β-gal)] in the developing postnatal retina revealed an expression pattern consistent with our current findings, as little to no β-gal signal was detected in perivascular cells [Ref. [61], and J. Chappell, unpublished data]. Because pericyte expression of *Flt1* and *Flk1* may be significantly lower relative to endothelial cells [27], additional analysis may be necessary to incorporate methods with enhanced sensitivities for Flt1 and Flk1 production and activity. Additionally, pericyte Flt1 may be more abundant at later developmental stages or in disease-specific contexts [28,31], beyond the early stages of vascular development that we observed herein. Thus, the apparent context-dependence for Flt1 synthesis from pericytes warrants further investigation to establish if this mode of VEGF-A regulation might be a potential therapeutic target in certain disease states.

Following their recruitment to the abluminal surface of developing vessels, perivascular cells migrate along the vasculature to establish sufficient coverage of the emerging vascular network [88,73]. Angiogenic endothelial cells secrete several molecular cues that modulate pericyte migration along the endothelium including PDGF-B, among others. For instance, Angiopoietin-2 (Angpt2) over-expression can induce pericyte migration off existing and remodeling vasculature [89], while Angpt1 promotes more stable interactions of pericytes with endothelial cells [90-92]. The Angpt-Tie pathway may also intersect with

heparin-binding EGF-like growth factor (HB-EGF) signaling [93], presumably through Erb1 and Erb4 receptors [94], to coordinate pericyte recruitment and subsequent migration along developing vessels. While our current data demonstrate how Flt1 regulation of VEGF-A influences downstream PDGF-B-PDGFRβ dynamics and subsequent pericyte coverage, we cannot rule out the influence of secondary effects from vessel dysmorphogenesis or the likely intersection(s) among a number of these collateral pathways, including the Angpt-Tie pathway [95]. In fact, additional transcriptional profiling and image analysis revealed that, in our ESC-derived vessel model, VEGF-A mis-regulation disrupted synthesis of important extracellular matrix (ECM) components such as Type IV Collagen (J. Darden and H. Zhao, unpublished data), which may play a critical role in pericyte migration dynamics. Additional studies are therefore essential for dissecting the unique contribution of these and other factors in regulating pericyte-endothelial cell interactions during the early stages of vessel formation as well as during vascular maturation.

The Notch pathway has emerged as a convergence point for many signaling pathways, most notable is the crosstalk with VEGF-A signaling in endothelial cells during sprouting angiogenesis [11-13]. Notch signaling in mural cells is also critical for vascular development, as disrupting Notch cues such as Jagged1 and Notch3 can compromise smooth muscle cell differentiation and investment [96,35,37]. Pericytes also appear to experience Notch signaling, though the downstream effects of Notch perturbations on pericytes are somewhat unclear, with pericyte *Pdgfrβ* expression and vessel coverage being affected in certain contexts [4,38,39] but not others [35-37,34]. In the current study,

embryonic pericytes stimulated by the Notch ligands Dll4 and Jag1 did not up-regulate *Pdgfrβ* expression, suggesting that the reduced expression of *Pdgfrβ* in pericytes was not directly downstream of the decreased endothelial expression of *Jag1* in the *Flt1*$^{-/-}$ ESC-derived vessels. In addition, pericyte coverage of ESC-derived vessels was not influenced by the addition of the Notch inhibitor DAPT. These observations are consistent with other embryonic vascular development studies in which loss of Notch signaling did not compromise pericyte PDGFRβ synthesis or pericyte coverage within the microcirculation [35,37]. Collectively our data, along with others, suggest that pericyte *Pdgfrβ* expression is Notch-independent in certain contexts. PDGFRβ activity may depend on alternate modes of regulation such as via other pathways e.g. Wnt or Transforming Growth Factor-β (TGFβ) signaling [97,98] or through a ligand-dependent feedback loop.

Pericyte coverage and stabilization of the developing vasculature requires competent PDGF-B signaling via full-length PDGFRβ on pericytes [99,16,43,100]. Interestingly, recent studies have suggested that perivascular cells may produce truncated PDGFRβ isoforms in certain scenarios like hypoxia, nutrient starvation, or rapid cellular proliferation [44-47,55]. Although less abundant in the *Flt1*$^{-/-}$ background, a PDGFRβ isoform shorter than full-length PDGFRβ (~60 kDa) was detected in pericytes from WT and *Flt1*$^{-/-}$ ESC-derived vessels. Sequence analysis suggested that this PDGFRβ isoform is presumably not the product of alternative splicing on the mRNA level, but rather from post-translational modification such as proteolytic cleavage, consistent with previous studies [45]. Receptor isoforms, particularly soluble ones, are a conserved element of numerous signaling pathways, including the VEGF-A axis [50,11,61], often functioning to regulate

ligand abundance and spatial distribution. It is therefore intriguing to speculate that this PDGFRβ isoform might also act in this way to modulate pericyte signaling, thereby "fine-tuning" vessel growth and maturation in certain contexts, such as in the germinal matrix regions of the developing brain [5]. If this or any other PDGFRβ isoforms are indeed functionally relevant, additional studies will be needed to establish the exact nature of their contribution to PDGF signaling and pericyte biology.

Given the importance of pericytes in promoting vascular stability and maturation throughout the human body [101-104,70], it is critical to expand our understanding of their basic behaviors during vessel development and specifically how different signaling pathways intersect to coordinate pericyte coverage of vascular networks. Here, we provided evidence for how mis-regulated VEGF-A activity impairs pericyte coverage and distribution by disrupting pericyte migration. The onset and progression of several pathological conditions such as cerebrovascular malformations (i.e. AVMs, CCMs, etc.), and neonatal germinal matrix hemorrhage involve a component of VEGF-A signaling occurring beyond a physiological range. The vascular abnormalities associated with these conditions result, in part, from downstream defects in pericyte behaviors and their underlying signaling mechanisms. Our data, along with others, suggest that therapeutic strategies designed to target Notch or PDGF-B signaling in pericytes will need to consider how a given disease context may alter or limit therapeutic efficacy via the effects of abnormal VEGF-A activity on pericyte responsiveness.

Acknowledgements

We thank the Chappell Lab for critical and extensive discussions of the primary data.

Funding: This study was funded by the National Institutes of Health (R00HL105779 and R56HL133826 to JCC).

Conflict of Interest: The authors declare that they have no conflict of interest.

FIGURE LEGENDS

Fig. 1 Genetic loss of *Flt1* impairs Ng2+ pericyte coverage of ESC-derived blood vessels. **A** Representative images of WT (i-iv) and *Flt1*$^{-/-}$ (v-viii) Day 9 ESC-derived blood vessels labeled for endothelial cells (Pecam1: i and v, green in iv and viii), pericytes (Ng2: ii and vi, red in iv and viii), and cell nuclei (DAPI: iii and vii, blue in iv and viii). Scale bars, 50 μm. **B** Average percentages of Ng2+ pericyte coverage on Days 9 (n=6 of biological replicates) and 10 (n=10 of biological replicates) ESC derived vessels for WT (black bars) and *Flt1*$^{-/-}$ (white bars) conditions. Values are averages + Standard Error of the Mean (SEM). *P≤0.05 vs. WT at the same time point

Fig. 2 *Flt1*$^{-/-}$ ESC-derived vessels display defects in pericyte distribution. **A** Schematic of ESC-derived vasculature with specific morphological locations denoted with dotted boxes: 1- vessel stalks, 2- branch points, and 3- thick areas. **B** Average number of Ng2+ pericytes at the indicated vessel locations within Day 9 WT (black bars, n=23 cells) and *Flt1*$^{-/-}$ (white bars, n=28 cells) ESC-derived vasculature. Values are averages + SEM. *P≤0.05 vs. WT at the same vessel location. **C** Percent distribution of pericytes at each vessel location (stalk: blue, branch point: red, thick area: gray) for Day 9 WT and *Flt1*$^{-/-}$ vessels (WT: n=158 cells, and *Flt1*$^{-/-}$: n=127 cells). *P=0.0002, Chi-square test of WT and *Flt1*$^{-/-}$ distributions. **D** Schematic of approach to quantifying pericyte density, specifically pericytes within a 50 μm radius of one another (dashed arrow and circle). **E** Average number of Ng2+ pericytes within a 50 μm radius of one another on Day 8-10 WT (black bars, Day 8: n=7, Day 9: n=23, Day 10: n=56) and *Flt1*$^{-/-}$ (white bars, Day 8: n=18, Day 9:

n=28, Day 10: n=53) ESC-derived vessels. Values are averages + SEM. *P≤0.05 vs. WT at Day 9 and Day 10, and **P≤0.05 for Day 8 WT vs. Day 10 WT.

Fig. 3 ESC-derived pericytes display little to no *Flt1* promoter activity or gene expression. **A** Representative images of Ng2+ pericytes (Ng2: i, red in iv and v) and *Flt1* promoter activity as indicated by β-galactosidase (β-gal: ii, blue in iv and v) production from the *Flt-1:LacZ* gene. Cell nuclei are labeled by DAPI (iii, white in v). Scale bar, 5 μm. **B** Fold change in *Flt1* expression between endothelial cells (yellow bar) and pericytes (purple bar) enriched from WT ESC-derived vessels. Values are averages + SEM, n=4 biological replicates. *P≤0.05

Fig. 4 Exogenous VEGF-A disrupts pericyte migration and limits pericyte distribution on developing embryonic blood vessels. **A** Representative sequential images from movies of vehicle control- (i-iii) and VEGF-A- (iv-vi) treated embryonic skin vessels in which endogenous pericytes (Ng2-DsRed+ and arrows, left column and red in right column) migrated along sprouting endothelial cells (Flk1-eGFP+ and arrowheads, middle column and green in right column). Time in upper right corner, hours:minutes (hh:mm). Scale bars, 100 μm. **B** Average percent of pericytes migrating on sprouts with directional persistence (tan bars) or static movement (dark blue bars) in control (n=23 movies) and VEGF-A-treated (n=15 movies) embryonic vessels. Values are averages + SEM. *P≤0.05. **C** Schematic of approach to quantifying pericyte density, specifically pericytes on sprouting endothelial cells within a 50 μm radius of one another (dashed arrow and circle).

D Average number of Ng2-DsRed+ pericytes within a 50 μm radius of one another in the first (black bars) and last (red bars) frames of movies from control (n=6 biological replicates) and VEGF-A-treated (n=4 biological replicates) embryonic vessels. Values are averages + SEM. *P≤0.05 vs. First Frames of VEGF-A-treated group

Fig. 5 Loss of *Flt1* disrupts transcriptional regulation within the Notch and PDGF-B pathways. **A** Fold change in Notch pathway gene expression between WT (dark blue bars) and *Flt1*$^{-/-}$ (yellow bars) endothelial cells enriched from ESC-derived vessels. Values are averages + SEM, n=4-8 biological replicates per gene. *P≤0.05 vs. WT. **B** Fold change in Notch pathway gene expression between WT (blue bars) and *Flt1*$^{-/-}$ (purple bars) pericytes enriched from ESC-derived vessels. Values are averages + SEM, n=4-8 biological replicates per gene. **C** Fold change in PDGF-B pathway gene expression between WT (dark blue bars) and *Flt1*$^{-/-}$ (yellow bars) endothelial cells enriched from ESC-derived vessels. Values are averages + SEM, n=4-8 biological replicates per gene. *P≤0.05 vs. WT. **D** Fold change in *Pdgfrβ* expression between WT (blue bars) and *Flt1*$^{-/-}$ (purple bars) pericytes enriched from ESC-derived vessels. Values are averages + SEM, n=4-8 biological replicates per gene. *P≤0.05 vs. WT

Fig. 6 *Flt1*$^{-/-}$ pericytes produce less PDGFRβ than WT pericytes, and pericytes in both backgrounds produce a truncated PDGFRβ isoform. **A** Representative images of Western Blots of recombinant PDGFRβ protein (top, antibody validation) and lysates from ESC-derived pericytes (bottom). Full-length (~180 kDa) and truncated (~60 kDa) isoforms of PDGFRβ were detected in WT and *Flt1*$^{-/-}$ pericyte lysates, and GAPDH (loading control)

was used to normalize and compare relative amounts of full-length PDGFRβ (0.29) and this truncated isoform (0.34) between groups. n=4 biological replicates. **B** Map of *Pdgfrβ* exons with important features denoted as well as arrows indicating the location of forward and reverse primers used to identify potential mRNA splice variants. **C** Representative image of *Pdgfrβ* amplicons separated on an agarose gel. Number ranges indicate PCR products within indicated primer sets. * indicates the presence of a potential mRNA splice variant.

Fig. 7 Immobilized Dll4, but not Jag1, induces changes in embryonic pericyte gene expression, but neither ligand alters *Pdgfrβ* expression. **A** Schematic of experimental setup for coating plates with Notch or control ligands, deriving Ng2-DsRed+ embryonic pericytes, and cultures these cells on Notch ligands to measure changes in gene expression. **B** Fold change in *Pdgfrβ* and Notch pathway gene expression between embryonic pericytes cultured under control conditions (black bars), exposed to Fc-γ and blocking serum only (white bars), on Fc-γ with Human Fc (gray bars), on Fc-γ with Dll4:Fc (red bars), or on Fc-γ with Jag1:Fc (light blue bars). Values are averages + SEM, n=5 biological replicates. *P≤0.05 vs. control conditions for specified gene target.

REFERENCES

1. Benjamin EJ, Blaha MJ, Chiuve SE, Cushman M, Das SR, Deo R, de Ferranti SD, Floyd J, Fornage M, Gillespie C, Isasi CR, Jimenez MC, Jordan LC, Judd SE, Lackland D, Lichtman JH, Lisabeth L, Liu S, Longenecker CT, Mackey RH, Matsushita K, Mozaffarian D, Mussolino ME, Nasir K, Neumar RW, Palaniappan L, Pandey DK, Thiagarajan RR, Reeves MJ, Ritchey M, Rodriguez CJ, Roth GA, Rosamond WD, Sasson C, Towfighi A, Tsao CW, Turner MB, Virani SS, Voeks JH, Willey JZ, Wilkins JT, Wu JH, Alger HM, Wong SS, Muntner P, American Heart Association Statistics C, Stroke Statistics S (2017) Heart Disease and Stroke Statistics-2017 Update: A Report From the American Heart Association. Circulation 135 (10):e146-e603. doi:10.1161/CIR.0000000000000485

2. Whitehead KJ, Smith MC, Li DY (2013) Arteriovenous malformations and other vascular malformation syndromes. Cold Spring Harb Perspect Med 3 (2):a006635. doi:10.1101/cshperspect.a006635

3. Leblanc GG, Golanov E, Awad IA, Young WL, Biology of Vascular Malformations of the Brain NWC (2009) Biology of vascular malformations of the brain. Stroke 40 (12):e694-702. doi:10.1161/STROKEAHA.109.563692

4. Kofler NM, Cuervo H, Uh MK, Murtomaki A, Kitajewski J (2015) Combined deficiency of Notch1 and Notch3 causes pericyte dysfunction, models CADASIL, and results in arteriovenous malformations. Sci Rep 5:16449. doi:10.1038/srep16449

5. Dave JM, Mirabella T, Weatherbee SD, Greif DM (2018) Pericyte ALK5/TIMP3 Axis Contributes to Endothelial Morphogenesis in the Developing Brain. Dev Cell. doi:10.1016/j.devcel.2018.01.018

6. Chappell JC, Bautch VL (2010) Vascular development: genetic mechanisms and links to vascular disease. Curr Top Dev Biol 90:43-72. doi:S0070-2153(10)90002-1 [pii]

10.1016/S0070-2153(10)90002-1

7. Vieira JM, Ruhrberg C, Schwarz Q (2010) VEGF receptor signaling in vertebrate development. Organogenesis 6 (2):97-106

8. Gerhardt H, Golding M, Fruttiger M, Ruhrberg C, Lundkvist A, Abramsson A, Jeltsch M, Mitchell C, Alitalo K, Shima D, Betsholtz C (2003) VEGF guides angiogenic sprouting utilizing endothelial tip cell filopodia. J Cell Biol 161 (6):1163-1177

9. Kappas NC, Zeng G, Chappell JC, Kearney JB, Hazarika S, Kallianos KG, Patterson C, Annex BH, Bautch VL (2008) The VEGF receptor Flt-1 spatially modulates Flk-1 signaling and blood vessel branching. J Cell Biol 181 (5):847-858. doi:jcb.200709114 [pii]

10.1083/jcb.200709114

10. Strilic B, Kucera T, Eglinger J, Hughes MR, McNagny KM, Tsukita S, Dejana E, Ferrara N, Lammert E (2009) The molecular basis of vascular lumen formation in the developing mouse aorta. Dev Cell 17 (4):505-515. doi:S1534-5807(09)00349-9 [pii]

10.1016/j.devcel.2009.08.011

11. Chappell JC, Mouillesseaux KP, Bautch VL (2013) Flt-1 (Vascular Endothelial Growth Factor Receptor-1) Is Essential for the Vascular Endothelial Growth Factor-Notch Feedback Loop During Angiogenesis. Arterioscler Thromb Vasc Biol 33 (8):1952-1959. doi:ATVBAHA.113.301805 [pii]

10.1161/ATVBAHA.113.301805

12. Jakobsson L, Bentley K, Gerhardt H (2009) VEGFRs and Notch: a dynamic collaboration in vascular patterning. Biochem Soc Trans 37 (Pt 6):1233-1236. doi:BST0371233 [pii]

10.1042/BST0371233

13. Siekmann AF, Covassin L, Lawson ND (2008) Modulation of VEGF signalling output by the Notch pathway. Bioessays 30 (4):303-313. doi:10.1002/bies.20736

14. Hellstrom M, Phng LK, Hofmann JJ, Wallgard E, Coultas L, Lindblom P, Alva J, Nilsson AK, Karlsson L, Gaiano N, Yoon K, Rossant J, Iruela-Arispe ML, Kalen M, Gerhardt H, Betsholtz C (2007) Dll4 signalling through Notch1 regulates formation of tip cells during angiogenesis. Nature 445 (7129):776-780. doi:nature05571 [pii]

10.1038/nature05571

15. Gerhardt H, Betsholtz C (2003) Endothelial-pericyte interactions in angiogenesis. Cell Tissue Res 314 (1):15-23. doi:10.1007/s00441-003-0745-x

16. Lindblom P, Gerhardt H, Liebner S, Abramsson A, Enge M, Hellstrom M, Backstrom G, Fredriksson S, Landegren U, Nystrom HC, Bergstrom G, Dejana E, Ostman A, Lindahl P, Betsholtz C (2003) Endothelial PDGF-B retention is required for proper investment of pericytes in the microvessel wall. Genes Dev 17 (15):1835-1840. doi:10.1101/gad.266803

17/15/1835 [pii]

17. Armulik A, Genove G, Mae M, Nisancioglu MH, Wallgard E, Niaudet C, He L, Norlin J, Lindblom P, Strittmatter K, Johansson BR, Betsholtz C (2010) Pericytes regulate the blood-brain barrier. Nature 468 (7323):557-561. doi:nature09522 [pii]

10.1038/nature09522

18. Daneman R, Zhou L, Kebede AA, Barres BA (2010) Pericytes are required for blood-brain barrier integrity during embryogenesis. Nature 468 (7323):562-566. doi:nature09513 [pii]

10.1038/nature09513

19. Stratman AN, Pezoa SA, Farrelly OM, Castranova D, Dye LE, 3rd, Butler MG, Sidik H, Talbot WS, Weinstein BM (2017) Interactions between mural cells and endothelial cells stabilize the developing zebrafish dorsal aorta. Development 144 (1):115-127. doi:10.1242/dev.143131

20. Hill RA, Tong L, Yuan P, Murikinati S, Gupta S, Grutzendler J (2015) Regional Blood Flow in the Normal and Ischemic Brain Is Controlled by Arteriolar Smooth Muscle Cell Contractility and Not by Capillary Pericytes. Neuron 87 (1):95-110. doi:10.1016/j.neuron.2015.06.001

21. Hall CN, Reynell C, Gesslein B, Hamilton NB, Mishra A, Sutherland BA, O'Farrell FM, Buchan AM, Lauritzen M, Attwell D (2014) Capillary pericytes regulate cerebral blood flow in health and disease. Nature 508 (7494):55-60. doi:10.1038/nature13165

22. Fernandez-Klett F, Potas JR, Hilpert D, Blazej K, Radke J, Huck J, Engel O, Stenzel W, Genove G, Priller J (2013) Early loss of pericytes and perivascular stromal cell-induced scar formation after stroke. J Cereb Blood Flow Metab 33 (3):428-439. doi:10.1038/jcbfm.2012.187

23. Hamilton NB, Attwell D, Hall CN (2010) Pericyte-mediated regulation of capillary diameter: a component of neurovascular coupling in health and disease. Front Neuroenergetics 2. doi:10.3389/fnene.2010.00005

24. Bergers G, Song S (2005) The role of pericytes in blood-vessel formation and maintenance. Neuro-oncology 7 (4):452-464. doi:10.1215/S1152851705000232

25. Kofler NM, Shawber CJ, Kangsamaksin T, Reed HO, Galatioto J, Kitajewski J (2011) Notch signaling in developmental and tumor angiogenesis. Genes Cancer 2 (12):1106-1116. doi:10.1177/1947601911423030

26. Schrimpf C, Teebken OE, Wilhelmi M, Duffield JS (2014) The role of pericyte detachment in vascular rarefaction. J Vasc Res 51 (4):247-258. doi:10.1159/000365149

27. Eilken HM, Dieguez-Hurtado R, Schmidt I, Nakayama M, Jeong HW, Arf H, Adams S, Ferrara N, Adams RH (2017) Pericytes regulate VEGF-induced endothelial sprouting through VEGFR1. Nature communications 8 (1):1574. doi:10.1038/s41467-017-01738-3

28. Cao R, Xue Y, Hedlund EM, Zhong Z, Tritsaris K, Tondelli B, Lucchini F, Zhu Z, Dissing S, Cao Y (2010) VEGFR1-mediated pericyte ablation links VEGF and PlGF to

cancer-associated retinopathy. Proc Natl Acad Sci U S A 107 (2):856-861. doi:0911661107 [pii]

10.1073/pnas.0911661107

29. He L, Vanlandewijck M, Raschperger E, Andaloussi Mae M, Jung B, Lebouvier T, Ando K, Hofmann J, Keller A, Betsholtz C (2016) Analysis of the brain mural cell transcriptome. Sci Rep 6:35108. doi:10.1038/srep35108

30. Fruttiger M (2002) Development of the mouse retinal vasculature: angiogenesis versus vasculogenesis. Invest Ophthalmol Vis Sci 43 (2):522-527

31. Shih SC, Ju M, Liu N, Smith LE (2003) Selective stimulation of VEGFR-1 prevents oxygen-induced retinal vascular degeneration in retinopathy of prematurity. J Clin Invest 112 (1):50-57

32. Matsumoto K, Azami T, Otsu A, Takase H, Ishitobi H, Tanaka J, Miwa Y, Takahashi S, Ema M (2012) Study of normal and pathological blood vessel morphogenesis in Flt1-tdsRed BAC Tg mice. Genesis 50 (7):561-571. doi:10.1002/dvg.22031

33. Luo L, Uehara H, Zhang X, Das SK, Olsen T, Holt D, Simonis JM, Jackman K, Singh N, Miya TR, Huang W, Ahmed F, Bastos-Carvalho A, Le YZ, Mamalis C, Chiodo VA, Hauswirth WW, Baffi J, Lacal PM, Orecchia A, Ferrara N, Gao G, Young-Hee K, Fu Y, Owen L, Albuquerque R, Baehr W, Thomas K, Li DY, Chalam KV, Shibuya M, Grisanti S, Wilson DJ, Ambati J, Ambati BK (2013) Photoreceptor avascular privilege is shielded by soluble VEGF receptor-1. Elife 2:e00324. doi:10.7554/eLife.00324

34. Liu H, Kennard S, Lilly B (2009) NOTCH3 expression is induced in mural cells through an autoregulatory loop that requires endothelial-expressed JAGGED1. Circ Res 104 (4):466-475. doi:CIRCRESAHA.108.184846 [pii]

10.1161/CIRCRESAHA.108.184846

35. Henshall TL, Keller A, He L, Johansson BR, Wallgard E, Raschperger E, Mae MA, Jin S, Betsholtz C, Lendahl U (2015) Notch3 is necessary for blood vessel integrity in the central nervous system. Arterioscler Thromb Vasc Biol 35 (2):409-420. doi:10.1161/ATVBAHA.114.304849

36. Pedrosa AR, Trindade A, Carvalho C, Graca J, Carvalho S, Peleteiro MC, Adams RH, Duarte A (2015) Endothelial Jagged1 promotes solid tumor growth through both pro-angiogenic and angiocrine functions. Oncotarget 6 (27):24404-24423. doi:10.18632/oncotarget.4380

37. Volz KS, Jacobs AH, Chen HI, Poduri A, McKay AS, Riordan DP, Kofler N, Kitajewski J, Weissman I, Red-Horse K (2015) Pericytes are progenitors for coronary artery smooth muscle. Elife 4. doi:10.7554/eLife.10036

38. Jin S, Hansson EM, Tikka S, Lanner F, Sahlgren C, Farnebo F, Baumann M, Kalimo H, Lendahl U (2008) Notch signaling regulates platelet-derived growth factor receptor-beta expression in vascular smooth muscle cells. Circ Res 102 (12):1483-1491. doi:10.1161/CIRCRESAHA.107.167965

39. Wang Y, Pan L, Moens CB, Appel B (2014) Notch3 establishes brain vascular integrity by regulating pericyte number. Development 141 (2):307-317. doi:10.1242/dev.096107

40. Geraldes P, Hiraoka-Yamamoto J, Matsumoto M, Clermont A, Leitges M, Marette A, Aiello LP, Kern TS, King GL (2009) Activation of PKC-delta and SHP-1 by hyperglycemia causes vascular cell apoptosis and diabetic retinopathy. Nat Med 15 (11):1298-1306. doi:10.1038/nm.2052

41. Abramsson A, Kurup S, Busse M, Yamada S, Lindblom P, Schallmeiner E, Stenzel D, Sauvaget D, Ledin J, Ringvall M, Landegren U, Kjellen L, Bondjers G, Li JP, Lindahl U, Spillmann D, Betsholtz C, Gerhardt H (2007) Defective N-sulfation of heparan sulfate proteoglycans limits PDGF-BB binding and pericyte recruitment in vascular development. Genes Dev 21 (3):316-331. doi:21/3/316 [pii]

10.1101/gad.398207

42. Hellstrom M, Gerhardt H, Kalen M, Li X, Eriksson U, Wolburg H, Betsholtz C (2001) Lack of pericytes leads to endothelial hyperplasia and abnormal vascular morphogenesis. J Cell Biol 153 (3):543-553

43. Hellstrom M, Kalen M, Lindahl P, Abramsson A, Betsholtz C (1999) Role of PDGF-B and PDGFR-beta in recruitment of vascular smooth muscle cells and pericytes during embryonic blood vessel formation in the mouse. Development 126 (14):3047-3055

44. Sagare AP, Sweeney MD, Makshanoff J, Zlokovic BV (2015) Shedding of soluble platelet-derived growth factor receptor-beta from human brain pericytes. Neurosci Lett 607:97-101. doi:10.1016/j.neulet.2015.09.025

45. Hutter-Schmid B, Humpel C (2016) Platelet-derived Growth Factor Receptor-beta is Differentially Regulated in Primary Mouse Pericytes and Brain Slices. Curr Neurovasc Res 13 (2):127-134

46. Mendelson K, Swendeman S, Saftig P, Blobel CP (2010) Stimulation of platelet-derived growth factor receptor beta (PDGFRbeta) activates ADAM17 and promotes metalloproteinase-dependent cross-talk between the PDGFRbeta and epidermal growth

factor receptor (EGFR) signaling pathways. J Biol Chem 285 (32):25024-25032. doi:10.1074/jbc.M110.102566

47. Duan DS, Pazin MJ, Fretto LJ, Williams LT (1991) A functional soluble extracellular region of the platelet-derived growth factor (PDGF) beta-receptor antagonizes PDGF-stimulated responses. J Biol Chem 266 (1):413-418

48. Hiratsuka S, Minowa O, Kuno J, Noda T, Shibuya M (1998) Flt-1 lacking the tyrosine kinase domain is sufficient for normal development and angiogenesis in mice. Proc Natl Acad Sci U S A 95 (16):9349-9354

49. Sawano A, Takahashi T, Yamaguchi S, Aonuma M, Shibuya M (1996) Flt-1 but not KDR/Flk-1 tyrosine kinase is a receptor for placenta growth factor, which is related to vascular endothelial growth factor. Cell Growth Differ 7 (2):213-221

50. Chappell JC, Cluceru JG, Nesmith JE, Mouillesseaux KP, Bradley V, Hartland C, Hashambhoy-Ramsay YL, Walpole J, Peirce SM, Gabhann FM, Bautch VL (2016) Flt-1 (VEGFR-1) Coordinates Discrete Stages of Blood Vessel Formation. Cardiovasc Res 111 (1):84-93. doi:10.1093/cvr/cvw091

51. Roberts DM, Kearney JB, Johnson JH, Rosenberg MP, Kumar R, Bautch VL (2004) The vascular endothelial growth factor (VEGF) receptor Flt-1 (VEGFR-1) modulates Flk-1 (VEGFR-2) signaling during blood vessel formation. Am J Pathol 164 (5):1531-1535

52. Taylor SM, Nevis KR, Park HL, Rogers GC, Rogers SL, Cook JG, Bautch VL (2010) Angiogenic factor signaling regulates centrosome duplication in endothelial cells of developing blood vessels. Blood 116 (16):3108-3117. doi:10.1182/blood-2010-01-266197

53. Zeng G, Taylor SM, McColm JR, Kappas NC, Kearney JB, Williams LH, Hartnett ME, Bautch VL (2007) Orientation of endothelial cell division is regulated by VEGF signaling during blood vessel formation. Blood 109 (4):1345-1352

54. Ho VC, Duan LJ, Cronin C, Liang BT, Fong GH (2012) Elevated vascular endothelial growth factor receptor-2 abundance contributes to increased angiogenesis in vascular endothelial growth factor receptor-1-deficient mice. Circulation 126 (6):741-752. doi:CIRCULATIONAHA.112.091603 [pii]

10.1161/CIRCULATIONAHA.112.091603

55. Hosaka K, Yang Y, Seki T, Nakamura M, Andersson P, Rouhi P, Yang X, Jensen L, Lim S, Feng N, Xue Y, Li X, Larsson O, Ohhashi T, Cao Y (2013) Tumour PDGF-BB expression levels determine dual effects of anti-PDGF drugs on vascular remodelling and metastasis. Nature communications 4:2129. doi:10.1038/ncomms3129

56. Kearney JB, Bautch VL (2003) In vitro differentiation of mouse ES cells: hematopoietic and vascular development. Methods Enzymol 365:83-98

57. Schindelin J, Arganda-Carreras I, Frise E, Kaynig V, Longair M, Pietzsch T, Preibisch S, Rueden C, Saalfeld S, Schmid B, Tinevez JY, White DJ, Hartenstein V, Eliceiri K, Tomancak P, Cardona A (2012) Fiji: an open-source platform for biological-image analysis. Nature methods 9 (7):676-682. doi:10.1038/nmeth.2019

58. Stegmuller J, Schneider S, Hellwig A, Garwood J, Trotter J (2002) AN2, the mouse homologue of NG2, is a surface antigen on glial precursor cells implicated in control of cell migration. J Neurocytol 31 (6-7):497-505

59. Zhao H, Darden J, Chappell JC (2018) Establishment and Characterization of an Embryonic Pericyte Cell Line. Microcirculation:e12461. doi:10.1111/micc.12461

60. Nesmith JE, Chappell JC, Cluceru JG, Bautch VL (2017) Blood vessel anastomosis is spatially regulated by Flt1 during angiogenesis. Development 144 (5):889-896. doi:10.1242/dev.145672

61. Chappell JC, Taylor SM, Ferrara N, Bautch VL (2009) Local guidance of emerging vessel sprouts requires soluble Flt-1. Dev Cell 17 (3):377-386. doi:10.1016/j.devcel.2009.07.011

62. Wild R, Klems A, Takamiya M, Hayashi Y, Strahle U, Ando K, Mochizuki N, van Impel A, Schulte-Merker S, Krueger J, Preau L, le Noble F (2017) Neuronal sFlt1 and Vegfaa determine venous sprouting and spinal cord vascularization. Nature communications 8:13991. doi:10.1038/ncomms13991

63. Krueger J, Liu D, Scholz K, Zimmer A, Shi Y, Klein C, Siekmann A, Schulte-Merker S, Cudmore M, Ahmed A, le Noble F (2011) Flt1 acts as a negative regulator of tip cell formation and branching morphogenesis in the zebrafish embryo. Development 138 (10):2111-2120. doi:138/10/2111 [pii]

10.1242/dev.063933

64. Zygmunt T, Gay CM, Blondelle J, Singh MK, Flaherty KM, Means PC, Herwig L, Krudewig A, Belting HG, Affolter M, Epstein JA, Torres-Vazquez J (2011) Semaphorin-PlexinD1 signaling limits angiogenic potential via the VEGF decoy receptor sFlt1. Dev Cell 21 (2):301-314. doi:S1534-5807(11)00267-X [pii]

10.1016/j.devcel.2011.06.033

65. Stefater JA, 3rd, Lewkowich I, Rao S, Mariggi G, Carpenter AC, Burr AR, Fan J, Ajima R, Molkentin JD, Williams BO, Wills-Karp M, Pollard JW, Yamaguchi T, Ferrara N,

Gerhardt H, Lang RA (2011) Regulation of angiogenesis by a non-canonical Wnt-Flt1 pathway in myeloid cells. Nature 474 (7352):511-515. doi:nature10085 [pii]

10.1038/nature10085

66. Greenberg JI, Shields DJ, Barillas SG, Acevedo LM, Murphy E, Huang J, Scheppke L, Stockmann C, Johnson RS, Angle N, Cheresh DA (2008) A role for VEGF as a negative regulator of pericyte function and vessel maturation. Nature 456 (7223):809-813. doi:nature07424 [pii]

10.1038/nature07424

67. Yamagishi S, Yonekura H, Yamamoto Y, Fujimori H, Sakurai S, Tanaka N, Yamamoto H (1999) Vascular endothelial growth factor acts as a pericyte mitogen under hypoxic conditions. Lab Invest 79 (4):501-509

68. Hagedorn M, Balke M, Schmidt A, Bloch W, Kurz H, Javerzat S, Rousseau B, Wilting J, Bikfalvi A (2004) VEGF coordinates interaction of pericytes and endothelial cells during vasculogenesis and experimental angiogenesis. Dev Dyn 230 (1):23-33. doi:10.1002/dvdy.20020

69. Larina IV, Shen W, Kelly OG, Hadjantonakis AK, Baron MH, Dickinson ME (2009) A membrane associated mCherry fluorescent reporter line for studying vascular remodeling and cardiac function during murine embryonic development. Anat Rec (Hoboken) 292 (3):333-341. doi:10.1002/ar.20821

70. Armulik A, Genove G, Betsholtz C (2011) Pericytes: developmental, physiological, and pathological perspectives, problems, and promises. Dev Cell 21 (2):193-215. doi:S1534-5807(11)00269-3 [pii]

10.1016/j.devcel.2011.07.001

71. Trotter J, Karram K, Nishiyama A (2010) NG2 cells: Properties, progeny and origin. Brain Res Rev 63 (1-2):72-82. doi:10.1016/j.brainresrev.2009.12.006

72. Attwell D, Mishra A, Hall CN, O'Farrell FM, Dalkara T (2016) What is a pericyte? J Cereb Blood Flow Metab 36 (2):451-455. doi:10.1177/0271678X15610340

73. Berthiaume AA, Grant RI, McDowell KP, Underly RG, Hartmann DA, Levy M, Bhat NR, Shih AY (2018) Dynamic Remodeling of Pericytes In Vivo Maintains Capillary Coverage in the Adult Mouse Brain. Cell reports 22 (1):8-16. doi:10.1016/j.celrep.2017.12.016

74. Fischer C, Mazzone M, Jonckx B, Carmeliet P (2008) FLT1 and its ligands VEGFB and PlGF: drug targets for anti-angiogenic therapy? Nat Rev Cancer 8 (12):942-956. doi:nrc2524 [pii]

10.1038/nrc2524

75. Arreola A, Payne LB, Julian MH, de Cubas AA, Daniels AB, Taylor S, Zhao H, Darden J, Bautch VL, Rathmell WK, Chappell JC (2018) Von Hippel-Lindau mutations disrupt vascular patterning and maturation via Notch. JCI Insight 3 (4). doi:10.1172/jci.insight.92193

76. Fong GH, Rossant J, Gertsenstein M, Breitman ML (1995) Role of the Flt-1 receptor tyrosine kinase in regulating the assembly of vascular endothelium. Nature 376 (6535):66-70

77. Armulik A, Abramsson A, Betsholtz C (2005) Endothelial/pericyte interactions. Circ Res 97 (6):512-523. doi:97/6/512 [pii]

10.1161/01.RES.0000182903.16652.d7

78. Kurup S, Abramsson A, Li JP, Lindahl U, Kjellen L, Betsholtz C, Gerhardt H, Spillmann D (2006) Heparan sulphate requirement in platelet-derived growth factor B-mediated pericyte recruitment. Biochem Soc Trans 34 (Pt 3):454-455. doi:10.1042/BST0340454

79. Liu ZJ, Shirakawa T, Li Y, Soma A, Oka M, Dotto GP, Fairman RM, Velazquez OC, Herlyn M (2003) Regulation of Notch1 and Dll4 by vascular endothelial growth factor in arterial endothelial cells: implications for modulating arteriogenesis and angiogenesis. Mol Cell Biol 23 (1):14-25

80. Harrington LS, Sainson RC, Williams CK, Taylor JM, Shi W, Li JL, Harris AL (2008) Regulation of multiple angiogenic pathways by Dll4 and Notch in human umbilical vein endothelial cells. Microvasc Res 75 (2):144-154. doi:S0026-2862(07)00080-5 [pii]

10.1016/j.mvr.2007.06.006

81. Beckstead BL, Santosa DM, Giachelli CM (2006) Mimicking cell-cell interactions at the biomaterial-cell interface for control of stem cell differentiation. J Biomed Mater Res A 79 (1):94-103. doi:10.1002/jbm.a.30760

82. Mouillesseaux KP, Wiley DS, Saunders LM, Wylie LA, Kushner EJ, Chong DC, Citrin KM, Barber AT, Park Y, Kim JD, Samsa LA, Kim J, Liu J, Jin SW, Bautch VL (2016) Notch regulates BMP responsiveness and lateral branching in vessel networks via SMAD6. Nature communications 7:13247. doi:10.1038/ncomms13247

83. Simonavicius N, Ashenden M, van Weverwijk A, Lax S, Huso DL, Buckley CD, Huijbers IJ, Yarwood H, Isacke CM (2012) Pericytes promote selective vessel regression to regulate vascular patterning. Blood 120 (7):1516-1527. doi:10.1182/blood-2011-01-332338

84. Kelly-Goss MR, Sweat RS, Stapor PC, Peirce SM, Murfee WL (2014) Targeting pericytes for angiogenic therapies. Microcirculation 21 (4):345-357. doi:10.1111/micc.12107

85. Gaengel K, Genove G, Armulik A, Betsholtz C (2009) Endothelial-mural cell signaling in vascular development and angiogenesis. Arterioscler Thromb Vasc Biol 29 (5):630-638. doi:ATVBAHA.107.161521 [pii]

10.1161/ATVBAHA.107.161521

86. Walpole J, Gabhann FM, Peirce SM, Chappell JC (2017) Agent-based Computational Model of Retinal Angiogenesis Simulates Microvascular Network Morphology as a Function of Pericyte Coverage. Microcirculation. doi:10.1111/micc.12393

87. Birbrair A, Zhang T, Wang ZM, Messi ML, Olson JD, Mintz A, Delbono O (2014) Type-2 pericytes participate in normal and tumoral angiogenesis. Am J Physiol Cell Physiol 307 (1):C25-38. doi:10.1152/ajpcell.00084.2014

88. Ando K, Fukuhara S, Izumi N, Nakajima H, Fukui H, Kelsh RN, Mochizuki N (2016) Clarification of mural cell coverage of vascular endothelial cells by live imaging of zebrafish. Development 143 (8):1328-1339. doi:10.1242/dev.132654

89. Hammes HP, Lin J, Wagner P, Feng Y, Vom Hagen F, Krzizok T, Renner O, Breier G, Brownlee M, Deutsch U (2004) Angiopoietin-2 causes pericyte dropout in the normal retina: evidence for involvement in diabetic retinopathy. Diabetes 53 (4):1104-1110

90. Patan S (1998) TIE1 and TIE2 receptor tyrosine kinases inversely regulate embryonic angiogenesis by the mechanism of intussusceptive microvascular growth. Microvasc Res 56 (1):1-21. doi:10.1006/mvre.1998.2081

91. Suri C, Jones PF, Patan S, Bartunkova S, Maisonpierre PC, Davis S, Sato TN, Yancopoulos GD (1996) Requisite role of angiopoietin-1, a ligand for the TIE2 receptor, during embryonic angiogenesis. Cell 87 (7):1171-1180

92. Jeansson M, Gawlik A, Anderson G, Li C, Kerjaschki D, Henkelman M, Quaggin SE (2011) Angiopoietin-1 is essential in mouse vasculature during development and in response to injury. J Clin Invest 121 (6):2278-2289. doi:10.1172/JCI46322

93. Iivanainen E, Nelimarkka L, Elenius V, Heikkinen SM, Junttila TT, Sihombing L, Sundvall M, Maatta JA, Laine VJ, Yla-Herttuala S, Higashiyama S, Alitalo K, Elenius K (2003) Angiopoietin-regulated recruitment of vascular smooth muscle cells by endothelial-derived heparin binding EGF-like growth factor. FASEB J 17 (12):1609-1621. doi:10.1096/fj.02-0939com

94. Stratman AN, Schwindt AE, Malotte KM, Davis GE (2010) Endothelial-derived PDGF-BB and HB-EGF coordinately regulate pericyte recruitment during vasculogenic tube assembly and stabilization. Blood 116 (22):4720-4730. doi:blood-2010-05-286872 [pii]

10.1182/blood-2010-05-286872

95. Uebelhoer M, Natynki M, Kangas J, Mendola A, Nguyen HL, Soblet J, Godfraind C, Boon LM, Eklund L, Limaye N, Vikkula M (2013) Venous malformation-causative TIE2 mutations mediate an AKT-dependent decrease in PDGFB. Hum Mol Genet 22 (17):3438-3448. doi:10.1093/hmg/ddt198

96. High FA, Lu MM, Pear WS, Loomes KM, Kaestner KH, Epstein JA (2008) Endothelial expression of the Notch ligand Jagged1 is required for vascular smooth muscle development. Proc Natl Acad Sci U S A 105 (6):1955-1959. doi:0709663105 [pii]

10.1073/pnas.0709663105

97. Cohen ED, Ihida-Stansbury K, Lu MM, Panettieri RA, Jones PL, Morrisey EE (2009) Wnt signaling regulates smooth muscle precursor development in the mouse lung via a tenascin C/PDGFR pathway. J Clin Invest 119 (9):2538-2549. doi:10.1172/JCI38079

98. Peng Y, Yan S, Chen D, Cui X, Jiao K (2017) Pdgfrb is a direct regulatory target of TGFbeta signaling in atrioventricular cushion mesenchymal cells. PLoS One 12 (4):e0175791. doi:10.1371/journal.pone.0175791

99. Bjarnegard M, Enge M, Norlin J, Gustafsdottir S, Fredriksson S, Abramsson A, Takemoto M, Gustafsson E, Fassler R, Betsholtz C (2004) Endothelium-specific ablation of PDGFB leads to pericyte loss and glomerular, cardiac and placental abnormalities. Development 131 (8):1847-1857. doi:10.1242/dev.01080

131/8/1847 [pii]

100. Lindahl P, Johansson BR, Leveen P, Betsholtz C (1997) Pericyte loss and microaneurysm formation in PDGF-B-deficient mice. Science 277 (5323):242-245

101. Kisler K, Nelson AR, Rege SV, Ramanathan A, Wang Y, Ahuja A, Lazic D, Tsai PS, Zhao Z, Zhou Y, Boas DA, Sakadzic S, Zlokovic BV (2017) Pericyte degeneration leads to neurovascular uncoupling and limits oxygen supply to brain. Nature neuroscience. doi:10.1038/nn.4489

102. Trost A, Lange S, Schroedl F, Bruckner D, Motloch KA, Bogner B, Kaser-Eichberger A, Strohmaier C, Runge C, Aigner L, Rivera FJ, Reitsamer HA (2016) Brain and Retinal Pericytes: Origin, Function and Role. Front Cell Neurosci 10:20. doi:10.3389/fncel.2016.00020

103. Sweeney MD, Ayyadurai S, Zlokovic BV (2016) Pericytes of the neurovascular unit: key functions and signaling pathways. Nature neuroscience 19 (6):771-783. doi:10.1038/nn.4288

104. Zhao Z, Nelson AR, Betsholtz C, Zlokovic BV (2015) Establishment and Dysfunction of the Blood-Brain Barrier. Cell 163 (5):1064-1078. doi:10.1016/j.cell.2015.10.067

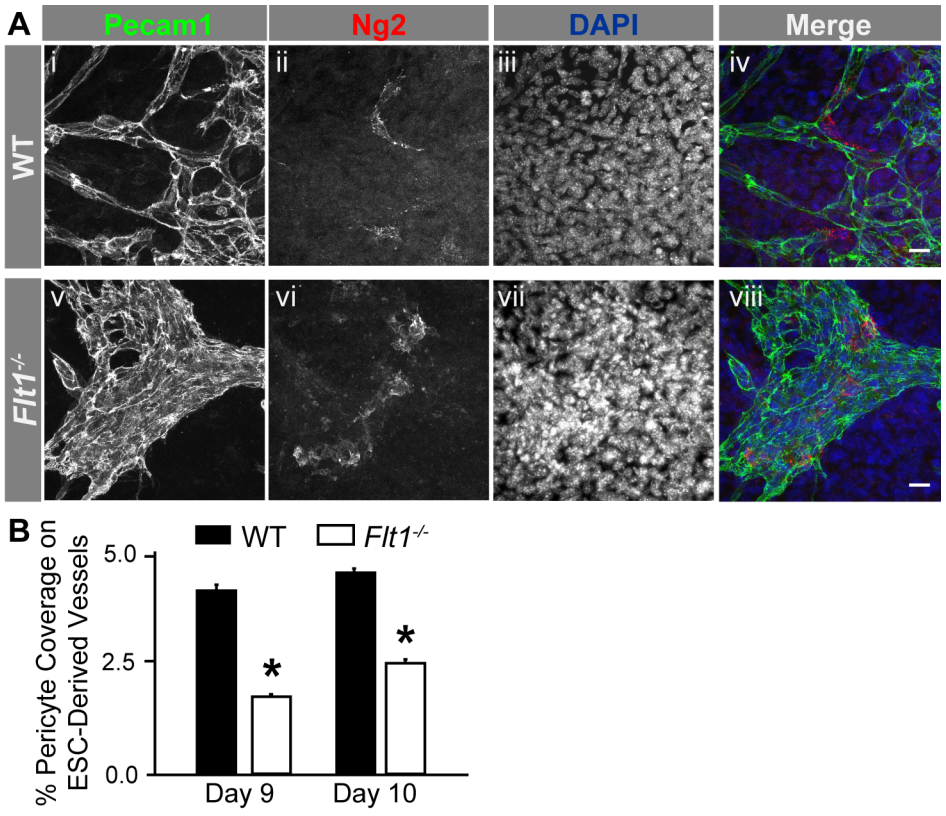
A
Pecam1
Ng2
DAPI
Merge
WT
Flt1-/-
i
ii
iii
iv
v
vi
vii
viii
B
WT
Flt1-/-
% Pericyte Coverage on ESC-Derived Vessels
5.0
2.5
0.0
*
*
Day 9
Day 10

Figure 1

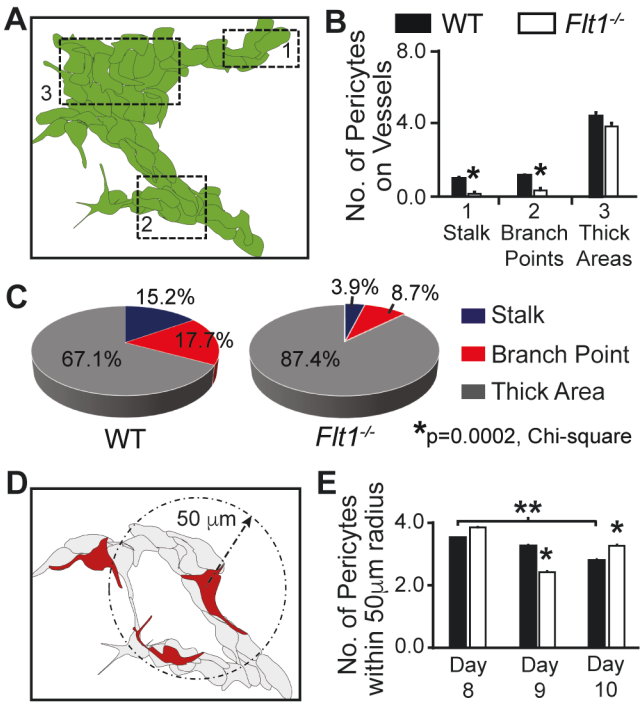
A
1
2
3
B
WT
Flt1-/-
No. of Pericytes on Vessels
8.0
4.0
0.0
*
*
1 Stalk
2 Branch Points
3 Thick Areas
C
15.2%
17.7%
67.1%
WT
3.9%
8.7%
87.4%
Flt1-/-
Stalk
Branch Point
Thick Area
*p=0.0002, Chi-square
D
50 μm
E
No. of Pericytes within 50μm radius
4.0
2.0
0.0
**
*
*
Day 8
Day 9
Day 10

Figure 2

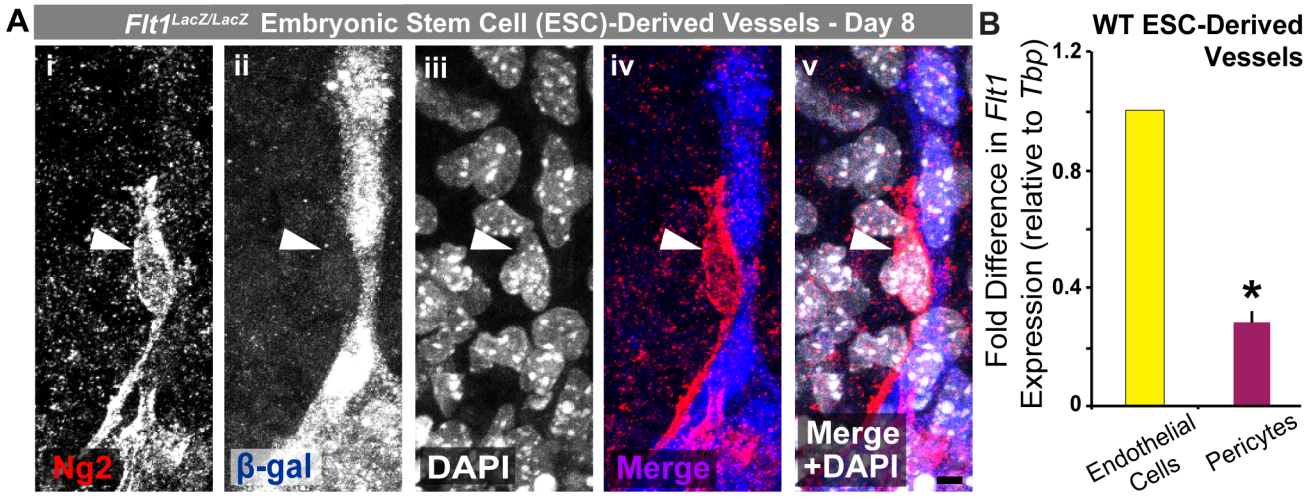
A
Flt1LacZ/LacZ Embryonic Stem Cell (ESC)-Derived Vessels - Day 8
i
ii
iii
iv
v
Ng2
β-gal
DAPI
Merge
Merge +DAPI
B
WT ESC-Derived Vessels
Fold Difference in Flt1 Expression (relative to Tbp)
1.2
0.8
0.4
0
*
Endothelial Cells
Pericytes

Figure 3

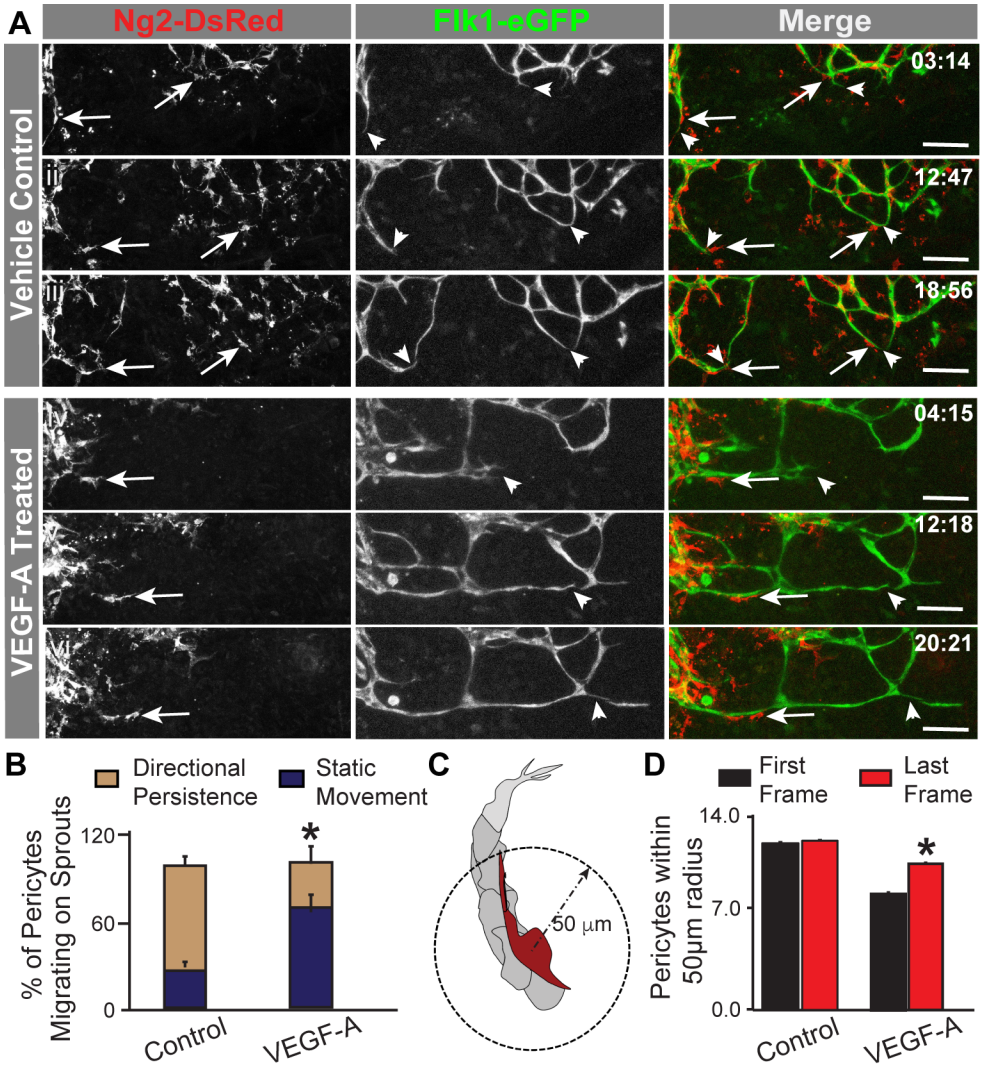
A
Ng2-DsRed
Flk1-eGFP
Merge
Vehicle Control
VEGF-A Treated
03:14
12:47
18:56
04:15
12:18
20:21
B
Directional Persistence
Static Movement
% of Pericytes Migrating on Sprouts
120
60
0
Control
VEGF-A
C
50 μm
D
First Frame
Last Frame
Pericytes within 50μm radius
14.0
7.0
0.0
Control
VEGF-A

Figure 4

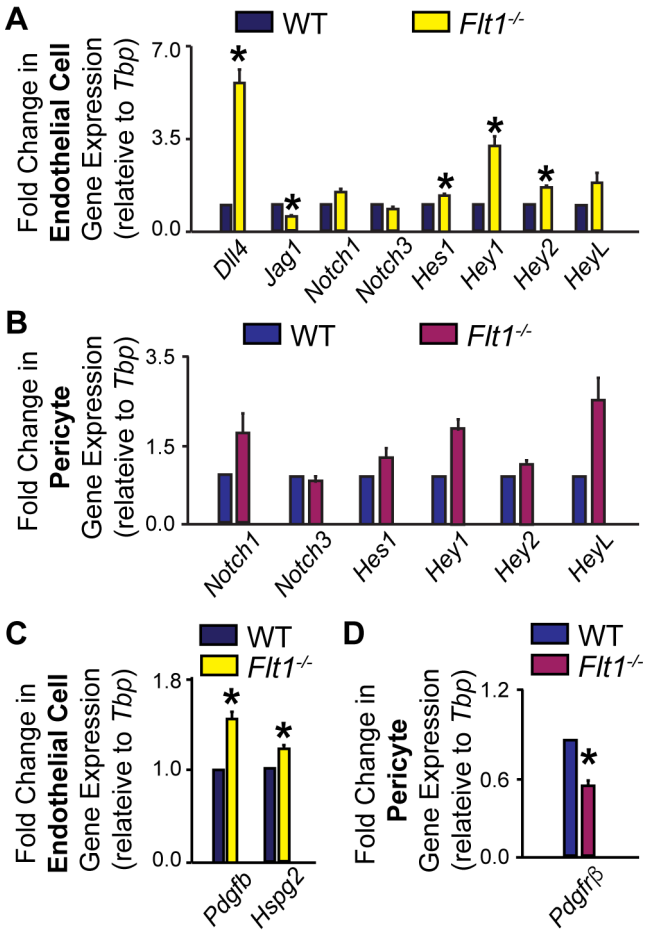
A
WT
Flt1-/-
Fold Change in Endothelial Cell Gene Expression (relateive to Tbp)
7.0
3.5
0.0
Dll4
Jag1
Notch1
Notch3
Hes1
Hey1
Hey2
HeyL
B
WT
Flt1-/-
Fold Change in Pericyte Gene Expression (relateive to Tbp)
3.5
1.5
0.0
Notch1
Notch3
Hes1
Hey1
Hey2
HeyL
C
WT
Flt1-/-
Fold Change in Endothelial Cell Gene Expression (relateive to Tbp)
1.8
1.0
0.0
Pdgfb
Hspg2
D
WT
Flt1-/-
Fold Change in Pericyte Gene Expression (relateive to Tbp)
1.2
0.6
0.0
Pdgfrβ

Figure 5

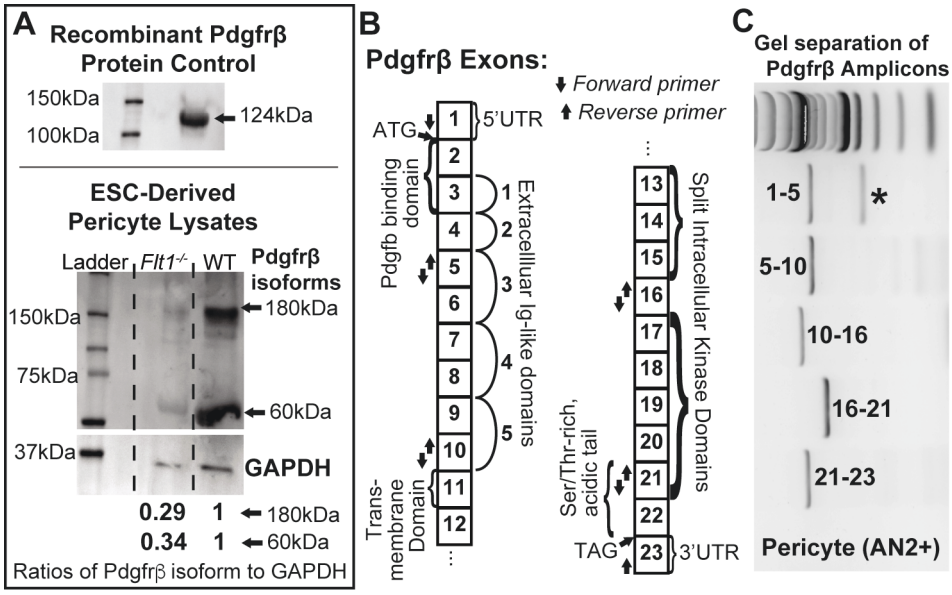
A
Recombinant Pdgfrβ Protein Control
150kDa
100kDa
124kDa
ESC-Derived Pericyte Lysates
Ladder
Flt1-/-
WT
Pdgfrβ isoforms
150kDa
75kDa
180kDa
60kDa
37kDa
GAPDH
0.29 1 180kDa
0.34 1 60kDa
Ratios of Pdgfrβ isoform to GAPDH
B
Pdgfrβ Exons:
Forward primer
Reverse primer
ATG
5'UTR
Pdgfb binding domain
Extracelllular Ig-like domains
Trans-membrane Domain
Split Intracellular Kinase Domains
Ser/Thr-rich, acidic tail
TAG
3'UTR
C
Gel separation of Pdgfrβ Amplicons
1-5
*
5-10
10-16
16-21
21-23
Pericyte (AN2+)

Figure 6

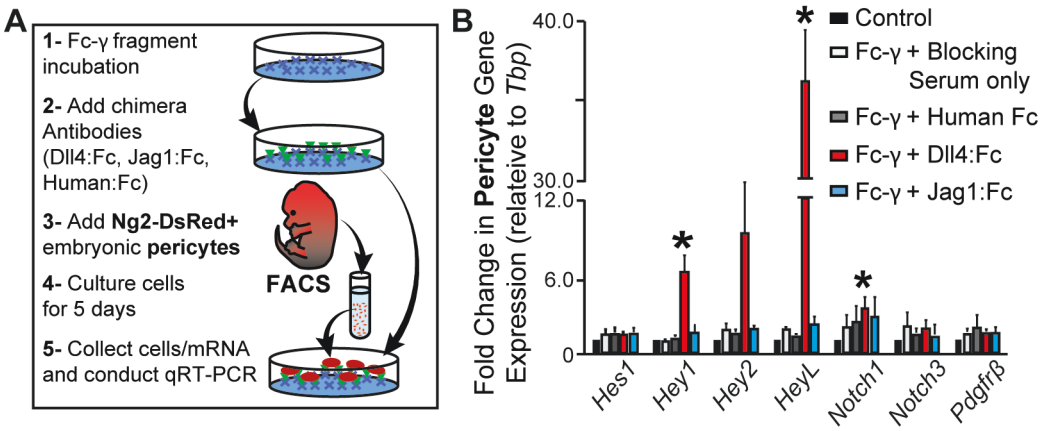
A
1- Fc-γ fragment incubation
2- Add chimera Antibodies (Dll4:Fc, Jag1:Fc, Human:Fc)
3- Add Ng2-DsRed+ embryonic pericytes
4- Culture cells for 5 days
5- Collect cells/mRNA and conduct qRT-PCR
FACS
B
Fold Change in Pericyte Gene Expression (relateive to Tbp)
40.0
30.0
12.0
6.0
0
Control
Fc-γ + Blocking Serum only
Fc-γ + Human Fc
Fc-γ + Dll4:Fc
Fc-γ + Jag1:Fc
*
Hes1
Hey1
Hey2
HeyL
Notch1
Notch3
Pdgfrβ

Figure 7